Phenological variation through time and space: its consequences for interspecific interaction and population dynamics

Takahashi, Kae

(Degree)
博士（理学）

(Date of Degree)
2019-03-25

(Date of Publication)
2020-03-01

(Resource Type)
doctoral thesis

(Report Number)
甲第7445号

(URL)
https://hdl.handle.net/20.500.14094/D1007445

博　士　論　文

Phenological variation through time and space: its consequences for interspecific interaction and population dynamics

フェノロジー時空間変異のメカニズムと帰結

：種間相互作用と個体群動態への影響

平成 31 年 1 月

神戸大学大学院理学研究科

髙　橋　華　江

Kae Takahashi

Contents

Summary

Phenology, the seasonal timing of life-history events, is a key for predicting distribution of organisms and population dynamics under fluctuating environments including recent climate change. Previous studies have found that phenology at population level varies through time and space, determining population dynamics and both the type and strength of interspecific interactions. Although causes and consequences of phenological variation on broad geographic scale have been well studied, those on relatively small spatial scale, where organisms forage or disperse, remain unknown. For example, when mature individuals have to disperse across local habitats to find their mates, spatial variation in reproductive phenology on regional scale, which consists of several local habitats, resulted in failure to find mate (reproductive asynchrony), which may influence population dynamics. Spatial variation of phenology would also cause unique interspecific interactions on small spatial scale. As another case, considering foraging movements of consumers among local habitats, consumers can extend their foraging opportunities by tracking the spatial variation of their resource phenology on regional scale because existence or suitable stages of the resources are temporally limited in each local habitat (phenological tracking). These unique consequences resulting from interactions between spatial variation in phenology and the movements of organisms have been overlooked in most of the previous studies conducted on broader scale. Although temperature have been increasing globally due to climate change, many inter-/intra-specific interactions would cause on more fine scale and the influence of global warming on organisms depend on spatial scale. Furthermore, the degree and/or patterns of the spatial variation might shift across years and influence population dynamics. Therefore, understanding phenological variation through time and

space is a key to deepen our understanding of the population dynamics and interspecific interactions under seasonal environments and to predict consequence of recent climate change for organisms. In this thesis, I explored causes of the annual and spatial variation in breeding phenology of the forest green tree frog, *Rhacophorus arboreus* and its consequences for interspecific interactions and population dynamics.

Few studies have quantified small-scale phenological variation and even few studies have explored factors determining the degree of the phenological variation. In Chapter 2, I surveyed breeding phenology of *R. arboreus* in 23 sites within Ashiu Forest Research Station on small spatial scale (< 10 km^2) across five years and clarified its potential underlying mechanism. Large spatial variation of phenological peaks (more than two weeks) among sites was observed every year. An accelerated failure time model suggested that site-specific and year-specific factors additively explained the spatiotemporal variation of phenology across five years. Randomization tests and annual variation of peak phenology in each site suggested that demographic stochasticity caused by population size might be a driving factor for the observed spatiotemporal variation. To the best of my knowledge, this is the first study to suggest that small population sizes are the driving factor for spatial variation in phenology on small spatial scale where environment conditions seem similar among local habitats. Demographic stochasticity may induce ecologically meaningful spatial variation in phenology, although the degree of demographic stochasticity might depend on other factors, such as environmental and/or genetic variations that are maintained in a certain region. Phenological variation on a small spatial scale may be more common than previously thought, because demographic stochasticity in phenology would cause regardless of species and habitat environments only if the population consist of small sub-populations. Moreover, the spatial variation of phenology might cause unique interspecific interactions on small spatial scale such as

phenological tracking.

The importance of temporal variation in phenology in determining specific interactions within single habitats has been increasingly recognized. However, it is not well known how spatial variation in phenology can mediate species interactions in spatially structured habitats. In Chapter 3, I demonstrated that the spatial variation of phenology of *R. arboreus* caused phenological tracking by a mobile predator of *R. arboreus* tadpole, the Japanese fire-bellied newt (*Cynops pyrrhogaster*) and the pattern of phenological tracking by newts determined the survival rate of *R. arboreus* using a spatially explicit semi-natural field mesocosm experiment. I hypothesized that when prey is exposed to a mobile predator, survival of the prey within a local habitat is strongly influenced by the degree of phenological synchrony with their conspecifics inhabiting an adjacent habitat. I showed that high degree of phenological synchrony of the prey between local habitats decreased the mean residence time of a newt in a local habitat. As a result, survival of the prey on a local habitat scale was higher in synchronous regions compared with the asynchronous regions even if both synchronous and asynchronous regions received same total prey inputs throughout the experimental period. Furthermore, variation in the ratio of residence time among individual newts explained the between-habitat variation of the tadpole survivals in synchronous region, suggesting that movement patterns of predators can mediate variation in local population dynamics of their prey. Although my experimental scale is much smaller than natural habitats and it would inevitably underestimate the movement cost of predators, this is the first study to experimentally demonstrate the importance of the relative timing (not the absolute timing) of prey phenology between local habitats in determining a prey-predator interaction in spatially structured environments. Given that predators usually forage within broader range than their preys' behavioral range, phenological tracking on small

spatial scale would be common phenomena. Since many studies have demonstrated that interspecific interactions caused by phenological matching can strongly determine individual fitness and population dynamics in a single habitat, it is necessarily to expect the spatial variation in phenology can further affect population dynamics in spatially structured habitats.

Previous studies have demonstrated that spatial variation in phenology on a relatively small spatial scale influence fitness components of organisms. Therefore, phenological variation through time and space might determine population dynamics in spatially structured habitats; however, this remains unknown. In Chapter 4, I demonstrated that spatial and annual variation in phenology can mediate long-term population dynamics using mathematical models. As dispersal among local populations is important factor in spatially structured habitats, metapopulation model is suitable to test the effects of spatial and temporal variation in phenology on the dynamics of spatial structured population. Matrix projection models were constructed to calculate the metapopulation dynamics of *R. arboreus* with spatial and annual variation in breeding phenology. I considered two metapopulation models, in which either habitat environment or demographic stochasticity is assumed as a driving factor of spatial variation. The environment model revealed that the spatial and temporal variations in phenology were important in determining metapopulation stability in the broad ranges of parameter setting. Interestingly, phenology of a given local population is influential for its dynamics and for determining the importance of dispersal in stabilizing the dynamics of a metapopulation. Moreover, demographic stochasticity revealed that metapopulation stability depended on the balance of migrations between populations, which was not found in the environment model. Considering that dispersal among local populations is common on small spatial scale, demographic stochasticity might influence metapopulation dynamics in spatially

structured habitats. Moreover, these results suggest it is important to identify the mechanisms underlying spatial and temporal variation in phenology to better understand population dynamics on a small spatial scale. These models are specific to the life history of *R. arboreus*. However, because both dispersal and differences in survival rate among habitats, caused by spatial variation in phenology, would be common in spatially structured habitats on small spatial scales, the results showing that phenological variation regulates metapopulation dynamics might be applied to other organisms; however, further research is needed.

Throughout this thesis, I emphasize the importance of considering phenological variation through time and space on small spatial to better understand the population dynamics and interspecific interactions. .

Chapter 1
General Introduction

To survive harsh environments, humans have studied the seasonal cycle of organisms, such as the fruiting of food plants and reproduction of predators, since the time of hunting and gathering societies. Now, scientists understand that the seasonal timing of life-history events, i.e., phenology, is a key for predicting organisms' distribution and population dynamics under fluctuating environments, including recent climate change (Post & Inouye 2008). Previous studies have found that the phenology at population level varies through time and space, determining population dynamics and both the type and strength of interspecific interactions (Yang & Rudolf 2010). In particular, the phenological peak of a certain population is an important characteristic because it influences its fate by determining overlap with other temporally varying environmental factors (Forrest & Miller-Rushing 2010).

In the temporal aspect, the phenology at population level of a species in a certain habitat varies annually partly because abiotic and biotic environmental factors fluctuate across over years (environmental stochasticity; Engen *et al.* 1998). Phenology at population level determines the survival rate and reproductive success of individuals each year, and hence, its population dynamics (Forrest & Miller-Rushing 2010; Yang & Rudolf 2010). Many researchers are interested in the effects of an annual shift in phenology on fitness components and population dynamics through interspecific interactions (Nakazawa & Doi 2012; Revilla *et al.* 2014). The temporal overlap of consumer food requirement and the resource availability determines the survival rates of both consumers and resource species (match-mismatch hypothesis; Durant *et al.* 2007).

In the spatial aspect, many studies have historically demonstrated phenological

variation among habitats on a geographic scale, such as latitude and altitude. For example, plant populations in cooler habitats at higher latitudes tend to undergo later leaf unfolding (Schwartz 1998) and earlier leaf fall than lower latitudes (Doi & Takahashi 2008). To compare phenological variation among habitats on a broad spatial scale, these studies have mainly explored environmental signals that determine phenology. Conversely, recent studies have demonstrated that phenology at population level considerably, even among neighboring habitats on a relatively small spatial scale (Post 2003; Uno & Power 2015). Phenological variation on a small spatial scale, at which individuals can forage or disperse within a generation, might have different consequences for population dynamics and intra-/interspecific interactions at local (i.e., one population) and regional scale (i.e., population consist of several local populations in a certain region). For example, when mature individuals have to disperse across local habitats to find their mates, spatial variation in reproductive phenology on a regional scale, which consists of several local habitats, resulted in failure to find a mate (reproductive asynchrony). Such spatial reproductive asynchrony influenced the population dynamics of gypsy moth, *Lymantria dispar* (L.) in North America (Walter *et al.* 2015). As another case, considering foraging movements of consumers among local habitats, consumers can extend their foraging opportunities by tracking the spatial variation of their resource phenology on a regional scale, because the existence or suitable stages of resources are temporally limited in each local habitat (phenological tracking; Deacy *et al.* 2016). These unique consequences resulting from interactions between spatial variation in phenology and the movement of organisms have been overlooked in most previous studies conducted on broader scales. Moreover, the causes of spatial variation in phenology remain unknown on a small spatial scale. Although temperatures have been increasing globally due to climate change, many inter-/intra-specific interactions would cause on more fine scale and the influence of

global warming on organisms depend on spatial scale (Levin 1992; IPCC 2007). For example, heterogeneity in the timing of plant growth decreased on a continental scale due to global warming but increased on a small spatial scale (meters to hundreds of meters; Post 2003; Post *et al.* 2008). Herbivores (*Rangifer tarandus*) tracked this spatial variation in the emergence phenology of resource plants, and this phenological tracking had marked effects on the reproductive success of *R. tarandus* each year. Furthermore, the degree and/or patterns of spatial variation might shift across years and influence population dynamics. Therefore, understanding phenological variation through time and space is key to our understanding of the population dynamics and interspecific interactions under seasonal environments, and to predict the consequence of climate change for organisms.

In this thesis, I demonstrate the causes and consequences of annual and spatial variation in breeding phenology of the forest green tree frog, *Rhacophorus arboreus* on a small spatial scale. In Chapter 2, I quantify annual and spatial variation in breeding phenology of *R. arboreus* populations for five years. In particular, I propose that a stochastic effect emerging from the population size would cause spatial variation in phenology within the study site. In Chapter 3, I demonstrate that spatial variation in breeding phenology of *R. arboreus* affected interspecific interactions between *R. arboreus* tadpoles and their predators Japanese fire-belied newt, *Cynops pyrrhogaster* by a field mesocosm experiment. When tadpoles were released at different times between the two habitats, which simulated reproductive asynchrony based on field observations, newts tracked the spatial variation in tadpole density and reduced the survival rate of the tadpoles than synchrony habitats. In Chapter 4, I examine how spatiotemporal variations in phenology affect population dynamics using mathematical models. The models I developed suggest that phenological variation caused by environmental factors and the stochastic effect would result in different consequences for population stability. Finally, I

discuss the generality of annual and spatial variation in phenology on a small spatial scale. Throughout this thesis, I emphasize the importance of considering phenological variation through time and space on small spatial scale to better understand the population dynamics and interspecific interactions.

Chapter 2
Annual and spatial variation in breeding phenology of *Rhacophorus arboreus*: testing a stochastic effect of population size

Introduction

Phenological variation on a relatively small spatial scale can have unique consequences on population dynamics and interspecific interactions, as described in Chapter 1. However, few studies have quantified such small-scale phenological variation and even fewer studies have explored factors determining the degree of phenological variation. Previous studies demonstrated that environmental factors, such as water, temperature, and elevation, vary to influence breeding phenology of sockeye salmon and gypsy moth, even on a small spatial scale (Régnière & Sharov 1998; Ruff *et al.* 2011). However, differences in environmental factors among local habitats should reduce as the spatial scale decreases (Moran 1953), which led us to expect that spatial variation in phenology should also reduce on smaller spatial scale. Contrary to this expectation, if there is obvious spatial variation in phenology, a stochastic factor mediated by population size may cause the variation. The phenology of individuals is determined by site-specific factors (such as environment) and individual factors such as genotype, which vary independent of the site an individual inhabits. The effect of individual timings of phenological events on population-level phenological parameters, such as peak timing, would increase with decreasing population size. Specifically, if individuals expressing early- or late-phenology are included in a small population, they may advance or delay the phenological peaks on a population-level. This stochastic process can generate spatial variation in phenology, especially when a regional population consists of small

subpopulations (hereafter “local population”). Such population structure is sometimes observed on a small spatial scale (e.g., Hanski *et al.* 1995). In conservation biology, “demographic stochasticity” is a well-known phenomenon, in which small populations are liable to become extinct because of large fluctuations in their population dynamics (Engen *et al.* 1998). Likewise, phenological variation on a small spatial scale might be determined by the demographic stochasticity. In this study, I define “demographic stochasticity in phenology” as a stochastic effect of local population size on the phenological peak of a population.

Demographic stochasticity in phenology would influence both the spatial variation in a single year and the annual variation. If demographic stochasticity strongly regulates spatial variation in phenology every year, the annual phenological shifts of small local populations would be larger than that of a large local population. The phenology of small populations would also shift annually without directivity (e.g., a habitat representing early phenology in one year can become a late phenology habitat in another year) and that of large populations would be relatively constant. As a result, demographic stochasticity would cause annual changes in spatial variation, especially for a regional population consisting of small local populations. Conversely, if the spatial variation of phenology on a regional scale is derived by the environmental factors, annual shifts of phenology for each local population would follow a similar trend. For example, if the phenological peak of each local population shift earlier by high air temperature, phenological peaks of all local populations would shift earlier in a warmer year, and the relative difference in phenology among local populations might be maintained across years (but see Post 2003). Differences in annual variation caused by demographic stochasticity and environmental factors may lead to differences in regional population dynamics (details in Chapter 4).

The forest green tree frog (*Rhacophorus arboreus*) is an endemic amphibian species in Japan. During an annual breeding season, a female spawns one foam nest on a tree branch, which is located above water. Therefore, the number of foam nests at each site indicate the population size of female in each site. Previous studies have shown that *R. arboreus* generally has a prolonged breeding period, which can last from April to July at individual breeding sites (Kato 1955, 1956). Tadpoles in a foam nest hatch within two weeks and drop into a pond with rain fall (Kusano *et al.* 2006). Japanese fire-bellied newt (*Cynops pyrrhogaster*) is a typical strong predator of *R. arboreus* tadpoles (Maeda & Matsui 1999). Previous research in a mountainous area identified 14 breeding sites on a small spatial scale (< 10 km^2) and their population size varied largely (3–104 foam nests, Takahashi & Sato 2015). Large spatial variation in peak timings was observed in a single year among these breeding sites (17.0 days in maximum), although altitude could not explain this spatial variation. Therefore, other effects, such as demographic stochasticity, are assumed to be potential driving factors of spatial variation in *R. arboreus* breeding phenology in this area.

The purpose of this study was to quantify spatial and annual variation in phenology on a small spatial scale and to clarify its potential underlying mechanism. To this end, I used the breeding phenology of *R. arboreus* to determine: (1) the degree of spatial variation on a small spatial scale across 5 years, (2) whether this variation in phenology is significantly different among years, populations, and population by year, (3) whether this spatiotemporal variation in phenology is larger than these population sizes expected, and (4) whether annual variation of phenological peaks in small local populations is larger than in large local populations. Overall, the results suggested that demographic stochasticity could be an important driving factor of observed annual and spatial variation of *R. arboreus* breeding phenology in the study site.

Method

Field observation

A field observation was conducted from May to August, from 2014 to 2018 in Ashiu Forest Research Station (AFRS), Kyoto University (35° 19′ N, 135° 43′ E). In AFRS, *R. arboreus* is a common amphibian species. In 5 years, I identified 23 breeding sites, which were small temporal ponds and marshes located in nearby streams (Table 1; Fig. 1). Newly spawned foam nests were recorded at each site every 1–15 days, during which most of the breeding season was covered in the study area; only 0–16 foam nests were found at the start day of observations and no foam nest was found on the last day of observations, except in 2014. When a new foam nest was found, it was marked with a small flag (length: 60 mm) to prevent the nest being counted twice. If the location of a foam nest was too high to place a flag, the nest was visually recorded using photos. These processes allowed me to count almost all foam nests spawned in each site. The area of sites was measured in the breeding seasons in 2017 and 2018. Air temperature in sites was measured using thermometers (KN Laboratories, Osaka, Japan) from May to September in each site in 2018. Water depth was measured at one to six locations in each site every three days in 2018.

Data Analysis

All statistical analyses were conducted in R 3.51 (Team & R Development Core Team 2016). To quantify spatial variation in phenology, the phenological peak of each site in each year was calculated as a median date. To test the extent of temporal and spatial variation in the breeding phenology of *R. arboreus*, an accelerated failure time model (AFT), which is a parametric survival analysis with a log-normal distribution, was used. In this model, the day of the year the foam nest was observed was used as a response

variable, while breeding sites, years, and their interactions were used as explanatory variables. Model selection by using the Akaike Information Criterion (Akaike 1987) was conducted to test whether phenological variation was due to the main effects of sites and years and their interaction effects. Relationships between phenological peaks of population and environmental factors were analyzed using data obtained in 2018. Mean temperature and mean water depth were used as environmental factors. Pearson's correlation tests were performed at a 0.05 level of significance.

The result of the AFT model is strongly influenced by large populations because of their large sample sizes (i.e., number of foam nests). Demographic stochasticity predicts that phenological peaks of large populations do not vary largely annually. Therefore, the AFT model might underestimate the effect of demographic stochasticity on the spatial variation in phenology in each year. Randomization tests were performed to assess how the spatial variation of phenological peaks in each year can be explained by demographic stochasticity considering population size. The principle of the test is to assess whether site-specific factors (such as the environment) make the observed phenological peaks in each population earlier or later than those predicted by the stochastic process that depends on population size. The null hypothesis suggests that the timing of individual breeding events is independent of the population it belongs to; thus, spatial variation of phenological peaks is caused by population size. In this test, wide variability in breeding dates is permitted for small populations under the null hypothesis. Although these randomization tests cannot directly show the effects of demographic stochasticity, the null hypothesis implies the effect of demographic stochasticity on the spatial variation. Specifically, phenological peaks in each population can be explained by demographic stochasticity without considering the effects of site-specific factors (see Discussion). To test for differences in phenological peaks among

populations, I calculated the phenological peak of each population in each year as a median date, as described above. To estimate the distribution of phenological peaks under the null hypothesis, I generated 10,000 new phenology data points per year by randomly permuting individual breeding dates within the whole study area. During the permutation process, I kept the total number of foam nests in the real population (i.e., population size) and the total number of foam nests in each observation day within the whole study area. In each permutation, the median date of breeding phenology for each population as a test statistic was built and two-sided tests with an alpha of 0.05 were conducted in each population.

To evaluate the extent of annual variation on phenological peaks in each site, the coefficient of variation (CV = standard deviation/mean) of the median date was calculated. The relationship between the mean population size and the CV of the median date across 5 years in each site was analyzed by Pearson's correlation tests at a 0.05 level of significance.

Results

In AFRS, the breeding phenology of *R. arboreus* was from 12 May (in 2015) to 13 August (in 2015). The total number of foam nests per year in AFRS ranged from 322 (in 2014) to 574 (in 2016), although this inter-annual variation might be caused by environmental fluctuations and by the frequency of field surveys. In fact, more foam nests were observed when more frequent surveys were performed: surveys were conducted every day and every seven days in 2016 and 2014, respectively. Larvae usually hatch in a foam nest approximately two weeks and then drop to the pond. However, disturbances such as wind, heavy rain, and predation by newts resulted in the collapse of foam nests in less than two weeks. Therefore, the number of foam nests would be underestimated when

field surveys were not frequent. However, excluding 2014, underestimation caused by the observation interval would be minimal, because foam nests were counted at least every three days in 2015, 2017, and 2018, and the total number of foam nests was not much lower (383, 490, and 564, respectively) than in 2016 (574), when foam nests were counted daily. The total annual number of foam nests at each site was highly correlated between years (Pearson correlation, $r = 0.93–0.98$).

The AFT model revealed that observed phenological variation was explained by the additive effects of sites and years. Interaction terms were dropped from the best model (Table 2; Fig. 2). The maximum spatial difference in peak phenology between sites ranged from 15.5 days in 2014 to 33.5 days in 2018. Even in 2018, when large spatial variation was observed, there was no clear relationship between environmental factors and phenological peak (mean temperature, Pearson correlation, $r = -0.11$, $p = 0.64$; mean water depth, Pearson correlation, $r = -0.23$, $p = 0.36$).

Randomization tests revealed that much of the observed phenology was not necessarily explained by site-specific factors. The null hypothesis was not rejected in 60.0–78.9% of cases in 2014–2018 (Table 3). Among 27 cases across five years, where the null hypothesis was rejected, the observed phenological peaks were significantly later than those generated under the null hypothesis in 24 cases, while the peaks were earlier in three cases.

The maximum annual variation in phenology peaks in each site across five years ranged from 2.5 days in site 12, to 23.0 days in site 5. The CV of the phenological peaks across five years ranged from 0.0065 in site 12, to 0.089 in site 13. The CV of smaller populations tended to be larger than that of larger populations, although the relationship was not statistically significant (Fig. 3, Pearson correlation, $r = -0.37$, $p = 0.11$).

Discussion

Although many studies have demonstrated spatial variation in phenology on a relatively large spatial scale, spatial variation on a small spatial scale has rarely been quantified despite its roles in mediating unique interspecific interactions and population dynamics. In this study, significant spatial variation in the breeding phenology of *R. arboreus* was observed on a small spatial scale over five years. Moreover, the analyses suggested that demographic stochasticity might be a driving factor for the observed spatiotemporal variation. Studies in conservation biology and population genetics have revealed the role of stochasticity in population dynamics (Bartlett 1960; Fréville *et al.* 2004) and trait divergence via genetic drift (Lofsvold 1988). However, demographic stochasticity has not been considered to influence spatial variation in phenology despite the theoretical evidence. To the best of my knowledge, this is the first study to suggest that small population sizes are the driving factor for spatial variation in phenology on a small spatial scale where environment conditions seem similar among local habitats. This spatiotemporal variation in breeding phenology might cause interspecific interactions such as phenological tracking (Chapter 3) and influence population dynamics (Chapter 4).

In the study area, large spatial variation of phenological peaks (more than 2 weeks) was observed every year. The best AFT model suggested that site-specific and year-specific factors additively explained the spatiotemporal variation of phenology across five years. However, because large populations have strong effects on the results of model selection, I was unable to test the effects of population size (i.e., demographic stochasticity) in the AFT model. To compensate for this statistical problem, randomization tests were conducted; these implied that a large extent of the spatial variation in phenology at population level each year can be explained without assuming

site-specific factors, such as the environment, of each site. Note that this does not mean that environmental factors did not affect phenology in each site. In reality, demographic stochasticity and environmental factors would simultaneously act to determine phenological variation. Temperature and water depth are important environmental factors for amphibian breeding phenology (Lane & Mahony 2002; Wells 2007). However, in 2018, these factors did not vary considerably among sites located on a relatively small spatial scale (~10 km^2), and did not explain the spatial variation of the phenological peaks in the simple correlation tests. Nevertheless, temporal changes in water depth may be important for breeding phenology in some sites. Specifically, site 23 is located in a dried marshland early in the breeding season in AFRS, and became a wet marsh later in the breeding season (Table 1). As the phenology of site 23 was significantly later than that predicted by the null hypothesis in 2016, 2017, and 2018 (Table 3), temporal elevation in water depth may be a signal for *R. arboreus* to begin breeding in this site.

Annual variation in peak phenology tended to increase with decreasing habitat size, which implies that population size can be a crucial factor determining the spatial variation in phenology. However, a simple correlation test did not reveal a significant relationship. This may be because environmental factors and demographic stochasticity would simultaneously drive spatial variation in each year. In fact, the results of the randomization test were not constant in five years; i.e., site-specific factors would regulate the phenological peak in some years, while demographic stochasticity was inferred in other years (Table 3). Thus, the relative importance of demographic stochasticity as a driving factor of spatial variation would vary between years. For example, spatial variation of phenology decrease during a low-precipitation year because of limited breeding opportunities. In such years, it may not be possible to detect demographic stochasticity even though it potentially drives spatial variation. Moreover, the regulation

of phenology in the whole study site by the biotic/abiotic environment, as well as genetic variation, would determine the effect of demographic stochasticity. If very low genetic variation for phenological traits is observed in the whole study site, demographic stochasticity occurring under phenological variation would be difficult to be detected. Further studies should explore the relationships between such factors and demographic stochasticity to test the generality of demographic stochasticity as a driving factor of spatial variation in phenology. Nevertheless, a large extent of variation in phenology can be explained without considering site-specific factors, which have been traditionally assumed by researchers to have large effects.

Ch.3
Spatial variation in prey phenology determines predator movement patterns and prey survival

Introduction

Variation in a species phenology influences the timing of ecological interactions with both abiotic and biotic environments, and thus is an important determinant of population dynamics, as well as the consequences of species interactions (Inouye 2008). While temporal variation in phenology is widely acknowledged to be an important factor determining species interactions within a local habitat (Durant *et al.* 2007; Rasmussen *et al.* 2015), how it influences species interactions when local habitats are spatially structured, a common environmental attribute in nature, has received less attention. Many studies have often focused on phenological variation on a species occurring across geographic scale (e.g., latitude or altitude). However, it has also become evident that the phenology of a species varies among habitats on relatively small spatial scale; e.g., timing of spawning salmon runs (Ruff *et al.* 2011; Koizumi & Shimatani 2016), aquatic insect emergence (Moore & Schindler 2010) and plants flowering (Post 2003).

In consumer-resource interactions, consumers can extend their foraging opportunities by tracking phenological variation of their resource species among local habitats (Lawson 1986; Fryxell *et al.* 2005; van Wijk *et al.* 2012). This phenological tracking by consumers can effectively reduce abundances of resource species on both local and regional scale, thus the spatial dimension of phenology can determine survival of resource species. The phenological tracking is common in nature, occurring among prey-predator (Schindler *et al.* 2013), plant-herbivore (Sawyer & Kauffman 2011), and plant–omnivore interactions (Coogan *et al.* 2012). For example, brown bears can track

spatial variation in peak spawning timing of salmon (Deacy *et al.* 2016). Similarly, female caribou (*Rangifer tarandus*) reproduce more offspring as the spatial variation in plant phenology increases (Post & Forchhammer 2008).

The efficiencies of phenological tracking by predators may in turn affect population structure and dynamics of their prey species, especially when prey are vulnerable to foraging only during a limited life stage (Yang & Rudolf 2010). Phenological synchrony among local habitats can be an adaptive strategy for resource species to reduce foraging pressure by mobile predators in spatially structured habitats (Ims 1990a). In general, reducing variation in reproductive phenology (known as reproductive synchrony) can facilitate predator satiation and consequently increase prey survival. When mobile predators forage in spatially structured environments included several segregated habitats, phenological synchrony among local habitats would also increase prey survival because individual predators can only forage in one of the local habitats at a given time. Therefore, the relative timing of prey species' phenology among local habitats, instead of its absolute timing, may have pronounced effects on their survival within and across local habitats in spatially structured habitats. Degree of phenological synchrony would determine phenological tracking of predator and feedback to prey survival. Theory has predicted whether the density dependent movements of predators can affect prey-predator interactions in spatially explicit models. However, the movement patterns of predator would be largely affected by other factors, for example energetic costs (Russell *et al.* 2003), trait variation among individuals (Nifong *et al.* 2014) and spatial memory (Merkle *et al.* 2014). Yet, no studies have empirically tested the movement pattern of predators mediated by phenological synchrony and their consequences on prey-predator interactions.

Prey-predator interaction between amphibian larvae and newts in riparian area

consisting of local habitats provides an excellent opportunity to test the above hypothesis. In Japanese riparian forests, forest green frogs (*Rhacophorus arboreus*) usually spawn at small ponds from May to July. Japanese fire-bellied newts (*Cynops pyrrhogaster*) are common predators for larvae (tadpoles) of *R. arboreus* (Maeda & Matsui 1999). Tadpoles are important but ephemeral resources for newts as they grow beyond the gape limit of newts within one month after hatching (K. Takahashi, unpublished data). Peaks of breeding phenology of *R. arboreus* vary considerably (3–20 days) among sites on a relatively small spatial scale (Chapter 2, Takahashi and Sato 2015), which creates a region consisting of sites with similar spawning timing (i.e., synchronous regions) or with different spawning timing (i.e., asynchronous regions). Consequently, prey availability in asynchronous regions may be higher than in synchronous regions because newts in asynchronous regions can prolong their foraging period on tadpoles by moving between nearby sites, each having eatable tadpoles at different timings (H. Matsuo & T. Sato, unpublished data).

Here I tested if the above scenario could mediate prey-predator interaction between tadpoles and an adult newt by using a semi-natural field experiment, in which the magnitude of tadpoles' phenological synchrony between two local habitats was directly manipulated (Fig. 4a and 4b). I specifically tested: (1) if newts can effectively track the phenological variation of their prey in asynchronous regions, whereas they represent variable movement patterns in synchronous regions because they have to make a choice among local habitats; (2) if survival of tadpoles becomes higher in local habitats in synchronous regions than in asynchronous regions, which is resulted from limited foraging opportunity for newts in the former region because tadpole become hard to be foraged as they grow; and (3) if a similar trend for the survival of tadpoles is detected on a regional scale. In synchronous regions, I expect that newts move between the two local

habitats in response to the temporal changes in prey densities in each habitat, which is assumed in a theory predicting the effects of mobile consumers on community dynamics (McCann *et al.* 2005). Alternatively, newts may stay longer in one local habitat than the other due to factors other than prey density. Such variations of consumer movements might determine heterogeneity of prey population dynamics among local habitats. Therefore, I further tested (4) if movement patterns of newts explain the variations in survival of tadpoles between the two local habitats in synchronous regions.

Materials and methods

Experimental design

The experiment was conducted from May to September 2014 in an open field at AFRS. I set enclosures consisting of two 60-L tanks, in which a newt can freely move between the two tanks to forage tadpoles (approximately 0.5 m apart, Fig. 4b, 4c and Fig. 5). To imitate synchronous regions in the enclosure, I added the tadpoles into two tanks simultaneously at early timing or late timing in synchronous treatment (hereafter, early-early treatment or late-late treatment). On the other hand, to create asynchronous region, I released tadpoles into two tanks at 23 days apart in asynchronous treatment (early-late treatment). The early timing corresponded to a peak of breeding phenology among all sites in this study region, whereas the late timing did to a peak of breeding phenology in some sites dominated by late spawners (Chapter 2, Takahashi & Sato 2015).

I created four treatments with 10 replicates (n = 40 treatment enclosures in total). The four treatments were as follows: (1) early-early treatment (EE), in which the two tanks in a treatment enclosure respectively received 200 tadpoles each synchronously (400 tadpoles in total) at the early timing of the frogs' breeding season (23 June, 2014); (2) late-late treatment (LL), in which the same number of tadpoles were introduced into

the two tank synchronously at the late timing (17 July, 2014); (3) early-late treatment (EL), in which the tadpoles were introduced into the two tanks asynchronously, i.e., 400 tadpoles in total per enclosure, but at 23 days apart between tanks; and (4) Control (CC), where no tadpoles were introduced into the two tanks in an enclosure. Here, tanks in each treatment were denoted by the combination of the treatment and the timing of tadpole addition. For example, a tank that was received tadpoles at the early timing in EL was denoted as 'EL-E'. At the five days before the tadpole addition at the early timing (i.e., 19 June), I released a newt into each treatment enclosure so as to acclimate the newt to the enclosure environment. Then, I examined the effects of phenological synchrony of tadpole phenology on the movement patterns of individual newts. Testing the effect of different input timing of tadpoles in synchronous treatments (i.e., EE vs LL) allowed me to test if the absolute phenological timing affected movement patterns of a newt and/or the survival of tadpoles. The control treatment was set to examine the movement patterns of a newt when there was no high quality resource.

To examine the survival of tadpoles under two extreme conditions of predator movement, I set additional two treatments with six replicates at both the early and late timing (n = 24 in total): first, a predator presence treatment (E_{p+} at the early timing and L_{p+} at the late timing), in which one newt was introduced into a tank having 200 tadpoles to simulate the local habitats where the newt stay resident; second, predator absence treatment (E_{p-} in the early timing and L_{p-} in the late timing), in which no newt was introduced into a tank having 200 tadpoles to simulate the local habitats with no predator arrival. I conducted the experiment on a relatively small spatial scale: i.e., 0.5m apart between the two local habitats (see detail in below). Although this distance corresponded to the shortest distance between sites in AFRS, it was much shorter than the ones commonly found in nature. Consequently, I inevitably underestimate the effects of

predator's movement costs on the results. However, the phenological tracking by mobile predator on relatively small spatial scale (suggesting low movement cost) have become increasingly evident (Armstrong *et al.* 2016), and therefore, I believe that testing my hypotheses would be important step to thoroughly understand prey-predator dynamics in spatially structured environments. I carefully discussed about this point in the Discussion.

Experimental setup

In early May, I developed the 40 enclosures and randomly assigned four treatments (EE, LL, EL and CC). The enclosures were made of a PVC frame (L × W × H = 1.5 × 1.0 × 0.5 m) covered by an open-top blue plastic tarp (Fig. 5, 6). In each enclosure, I placed two 60-L tanks (L × W × H = 0.7 × 0.4 × 0.2 m) approximately 0.5 m apart (0.48 ± 0.05 m in SD). The two tanks were bridged by a folding plastic net (10 mm in mesh size) flattened on the enclosure-ground, which allowed newt movement between the two tanks. I made a drain at a 15 cm height of each tank to maintain a tank with 40L of water. For predator presence/absence treatments, I made additional 12 enclosures and equally divided each enclosure into two parts (L × W × H = 0.75 × 1.0 × 0.5 m; 24 small enclosures in total) by adding PVC frames with a plastic tarp. Then, I randomly assigned predator presence and absence treatments to the small enclosures. A 60-L tank was located at the center of each small enclosure, which resulted in keeping a number of tanks per area of an enclosure among all treatments. A half-size of a folding plastic net was installed in each tank, which allowed newts to move between inside and outside of a tank and allowed tadpoles to have an equivalent tank structure with those in other phenology treatments. All enclosures were covered by an 80%-shading net to simulate a natural environment having a moderate level of canopy cover. The shading net also limited immigration of terrestrial/aquatic invertebrates that could result in an unexpected

variation of prey resources for newts among treatments.

I filled each tank with 10 L river water on 16 May, followed by 200 mL of benthic mud filtered through 2.0 mm mesh on 19 May. This led to colonization of microbes, periphyton and benthic invertebrates. Microbes, periphyton and dead invertebrates were potential prey for tadpoles, while living benthic invertebrates were prey for newts. Since I used river water and natural mud from ponds in AFRS, I did not add nutrients artificially.

On 19 June, I released one adult male newt (Snout-vent length, 53.1 ± 2.5 mm in SD) at the center of each enclosure. After an acclimation for the newts in the enclosures for five days, 200 tadpoles of *R. arboreus* (stage 25, Snout-vent length, 7.1 ± 1.2 mm in SD, Gosner 1960; stage 34, Iwasawa and Kawasaki 1979) were introduced into a tank assigned as the early timing on

The date of 24 June was an onset of the experiment. I released another 200-tadpoles into a tank assigned as the late timing on 17 July (i.e., 24 days apart between the early and late timing) (Snout-vent length, 6.3 ± 1.1 mm). The density of tadpoles (714 tadpoles m^{-2}) was within the range of natural densities of the tadpoles in the study region (21-1645 tadpoles m^{-2}). Hereafter, I referred a period from 24 June to 16 July as early period (23 days) and a period from 17 July to 9 August as late period (24 days). At the end of the late period, the number of tadpoles decreased by one-day was very low (LL-L and EL-L in 10 August, 3.1 ± 3.2), suggesting that the effect of one-day difference between the early and late periods on the result was negligible.

Data collections

To examine the movement patterns of newts, I recorded a location (tank ID or outside of tank) of a newt in each enclosure once a day (from evening toward night time: 5-11 pm) throughout the experiment, except during extreme weather conditions (5 days).

The newts were observed outside the tanks less frequently throughout the experiment (≈ 2.1 and ≈ 5.7 days in the early and late periods, respectively) and hence I only used the number of days that the newts stayed in each tank. When the newt could not be found for more than 3 days, I regarded the newt escaped from the enclosure and added a new newt with similar body size and weight (9 cases in total throughout the experiment).

To examine the number of tadpoles in each tank, I recorded images of each tank with a digital camera (Olympus TG-830, Olympus corporation, Tokyo, Japan) at the end of the early period (16 July), the late period (9 August) and 23 days after the end of the late period (1 September), and counted the number of tadpoles by using ImageJ v1.48 (Schneider *et al.* 2012). During 23 days after the late period, I maintained the experimental conditions in each enclosure, including the newt and other environmental setting. I counted the number of tadpoles at 23 days after the end of the late period to examine if the total survival in EL and LL were overestimated relative to EE due to the arbitrary defined timing (at the end of the late period), i.e., tadpoles introduced at the late period had experienced predation only for 24 days (the late period), whereas tadpoles introduced at the early period experienced it for 47 days (the early period + the late period). I examined body size of individual tadpoles in each tank at the end of each period. To this end, I collected approximately 30 tadpoles in each tank, took photo images, and then measured body size by using the ImageJ. The collected tadpoles were released in each tank.

To examine background ecosystem properties, I measured nutrient availability, gross primary productivity (GPP), and periphyton biomass of each tank at the end of each period. Filtered water samples (Whatman GF/F) were collected from all tanks at July 6 and July 30, stored on ice in the field, and then frozen in the laboratory until analysis. The concentrations of ammonium (NH_4^+), nitrate (NO_3^-) and phosphorus (PO_4^{3-}) were

analyzed with a Bran + Luebee AutoAnalyzer III (BLTEC, Osaka, Japan). GPP was measured at July 6 and July 30 using diurnal changes in oxygen levels (Wetzel & Likens 1991). Dissolved oxygen (DO) measurements were conducted by using an oxygen probe DO-31P (DKK-TOA corporation, Tokyo, Japan) three times per sampling period: at sunrise (t_0), sunset (t_1) and the following sunrise (t_2). Net primary productivity (NPP) was calculated as DO (t_1) - DO (t_0), community respiration (CR) as DO (t_1) - DO (t_2), and GPP as NPP + CR. To estimate periphyton biomass, I sampled tiles in each tank (two tiles per collection) on 9 and 31 July. The two ceramic tiles (1.8 × 1.8 cm) were placed in an open-top plastic food container (10 cm in diameter with 4 cm height) with two windows (L × W = 6 × 2 cm) that allowed tadpoles to forage periphyton within a container. The container floated with attached polystyrene, which prevented sedimentation on the tiles, allowing periphyton to grow. The tiles were preserved at a freezer for approximately 12 weeks, and chlorophyll a content was measured according to a standard method (Steinman *et al.* 2006).

Statistical analysis

All statistical analyses were conducted in R v3.10 (Team & R Development Core Team 2016), with an alpha of 0.05. I used generalized linear models (GLMs) to test whether movement patterns of predators and prey survival were affected by a relative timing of prey phenologies between local habitats, absolute timing of prey phenologies and their interaction. Specifically, the relative timing was defined by the synchrony term (i.e., synchrony or asynchrony), while the absolute timing was defined by the period term (the early period or the late period). This resulted in four types of tanks across treatments (synchrony/asynchrony × early/late): EE-E, a tank with tadpole addition at the beginning of the early period in a synchronous treatment (n = 20 tanks); LL-L, a tank with tadpole

addition at the beginning of the late period in a synchronous treatment (n = 20); EL-E, a tank with tadpole addition at the beginning of the early period in an asynchronous treatment (n = 10); EL-L, a tank with tadpole addition at the beginning of the late period in an asynchronous treatment (n = 10). Then, I tested the effects of the relative timing, absolute timing and their interaction on residence time of the predatory newts and survival of the tadpoles in each tank, respectively: e.g., glm (residence time ~ period + synchrony + P:S + error). Since the number of tadpoles added into each tank was same across treatments, I considered the survival simply as the number of tadpoles survived during each sampling period. I used negative binomial distribution and log link function in the GLMs. I also tested if the residence time of the newts, period and their interaction can explain the variations in the tadpole survival in each tank by using another GLM: glm (no. of tadpole ~ residence time + period + R:P + error). I evaluated significance of fixed effects and their interactions by using a type II ANOVA with the log-likelihood ratio test (R package 'car'). Type II ANOVAs obeyed the marginality principle and tested each term in the model after all others, except for the term's higher-order relatives (Fox & Weisberg 2011).

I also hypothesized that newt movement patterns would explain variation in the survival of tadpoles between the two habitats in synchronous treatments. To test that, the relationship between the ratio of newt's residence time between two habitats in an enclosure and the ratio of tadpole survivals between the two tanks in the enclosure was evaluated for each period by using Spearman's rank correlation test. Note that an escaped newt from a synchronous treatment in the late period (LL) resulted in reduced sample size (n = 9).

I examined the total number of tadpoles survived in each enclosure (as a surrogate measure of prey survival on regional scale) at the end of the late period, as well

as 23 days after the end of the late period. The GLM with negative binomial distribution and log-link function was used to test the treatment effect on the total number of surviving tadpoles. If a treatment effect was found, the pairwise difference between treatments (EE vs. LL vs. EL) was tested using Tukey's comparison with the 'multcomp' package in R.

Results

As I expected, the relative timing (i.e., synchrony vs. asynchrony) of tadpole additions between the two tanks within an enclosure strongly affected the residence time of newts in each tank ($\chi^2 = 20.3$, $p < 0.001$; Fig. 7). That is, residence time of the newts was, on average, longer in tanks with tadpoles in asynchronous treatments (i.e., EL-E in the early period and EL-L in the late period; Fig. 4c) than tanks in synchronous treatments (i.e., EE-E in the early period and LL-L in the late period). Residence time was longer in the early period than in the late period, indicating that there was also a significant effect of the absolute timing ($\chi^2 = 4.0$, $p = 0.04$). The interaction between the relative timing and period was not significant ($\chi^2 = 0.001$, $p = 0.97$), meaning that the effect of relative timing did not depend on the periods (i.e., early or late). The newts in control treatment had similar residence times with those found in synchronous treatments in both periods.

The effect of the relative timing of tadpole addition on the movement pattern of newt affected the survival of tadpoles. Specifically, the mean number of tadpoles surviving in a tank was larger in synchronous treatment than in asynchronous treatment ($\chi^2 = 11.8$, $p < 0.001$; Fig. 8). While the newts tended to stay longer time in tanks in the early period than in the late period, more tadpoles survived in the early period than in the late period ($\chi^2 = 9.5$, $p = 0.002$). Furthermore, the effect of the relative timing on the number of tadpoles surviving was stronger in the early period than the late period (relative timing × period: $\chi^2 = 4.2$, $p = 0.04$). Survival of tadpoles was higher in the early period

than in the late period in predator presence treatment (E_{p+} vs L_{p+}: $\chi^2 = 10.9$, $p < 0.001$). Natural mortality rate was higher in the late period than in the early period (E_{p-} vs. L_{p-}: $\chi^2 = 31.5$, $p < 0.001$).

Tadpole survival decreased with increasing the resident time of newts ($\chi^2 = 41.4$, $p < 0.001$; Fig. 9). This trend was more pronounced in the early period than in the late period (residence time × period, $\chi^2 = 7.4$, $p = 0.006$). In synchronous treatments, the ratio of the newt's residence time between two tanks was close to 1.0 on median (EE in the early period: 0.76; LL in the late period: 0.9), suggesting the newts foraged two tanks equally within an enclosure on average. However, some individuals stayed much longer in one tank than in the other even in the synchronous treatment (Maximum: 19 vs. 2 days in an enclosure in the early period; 16 vs. 2 days in the late period). Consequently, the ratio of the newt's residence time varied among individuals, and I found that the ratio was positively correlated with the ratio of tadpole survivals between two tanks within an enclosure in the early period (Spearman's $r = -0.88$, $p < 0.001$, $n = 10$; Fig. 10). However, no such correlation was found in the late period (Spearman's $r = -0.12$, $p = 0.74$, $n = 9$).

Contrary to my expectation, the effects of the relative timing of tadpole addition on the survival of tadpoles in tanks (local habitat scale) were not translated into the total survival in each enclosure (regional scale). Specifically, the total number of tadpoles surviving differed significantly among treatments at the end of the late period ($\chi^2 = 41.6$, $p < 0.0001$; Fig. 11). The multiple comparisons test revealed that the total survival of tadpoles was higher in treatments that experienced the tadpole addition in the late period (i.e., EE < EL < LL; EE vs EL, $z = -3.3$, $p = 0.003$; LL vs EL, $z = 3.3$, $p = 0.003$; EE vs LL, $z = 6.5$, $p < 0.001$). Until 23-days after the completion of the late period, the total number of tadpoles in late-synchronous treatment and asynchronous treatment declined quickly, and no significant difference among treatments were found ($\chi^2 = 3.2$, $p = 0.20$).

I expected that the efficiencies of the phenological tracking by newts should be high if the tadpoles grew fast and were vulnerable to newts' predation only during a limited period due to the gape limit of newts. In relevant to this, body size of tadpoles was small across treatments and less variable among treatments (the early period: 8.30–9.16 mm in mean snout-vent length among treatments, the late period: 7.86–8.52 mm; Fig. 12), suggesting low growth rates of tadpoles in this experiment. Consequently, only 19 metamorphosed frogs were found across all treatments until 23 days after the end of the late period [n = 12 in early-synchronous treatment (EE-E), one in early-predator presence treatment (E_{P+}), four in early-predator absence treatment (E_{P-}), and two in late-predator absence treatment (L_{P-})]. NH_4^+, NO_3^- and PO_4^{3-} were respectively 0.02–0.96 mg L^{-1}, 0.07–1.18 mg L^{-1} and 0.004–0.10 mg L^{-1} across treatments throughout the experiment (Fig. 13, 14, 15). GPP was 0.04–1.26 mg O_2 L^{-1} h^{-1} across treatments throughout the experiment (Fig. 16). Finally, periphyton biomasses, main resource for the tadpoles, were 1.28–10.42 mg cm^{-2} across treatments throughout the experiment (Fig. 17).

Discussion

The importance of temporal variation in phenology in determining specific interactions within local habitats has been increasingly recognized (Durant *et al.* 2007; Yang & Rudolf 2010). However, it is not well known how spatial variation in phenology can mediate species interactions in spatially structured environments (Post *et al.* 2008). In this study, I hypothesized that when exposed to a mobile predator, survival of prey within a local habitat is strongly influenced by phenological synchrony with their conspecifics inhabiting an adjacent habitat. By using spatially explicit semi-natural field experiment, I showed that phenological synchrony of prey (tadpoles of *R. arboreus*) between local habitats (i.e., tanks) decreased the mean residence time of a predator (newt,

C. pyrrhogaster) in a local habitat. As a result, survival of prey on a local habitat scale was higher in synchronous regions compared with the asynchronous regions even if both synchronous and asynchronous regions received same total prey inputs throughout the experimental period. Furthermore, variation in the ratio of residence time among individual newts explained the between-habitat variation of the tadpole survivals in synchronous region, suggesting that movement patterns of predators can mediate variation in local population dynamics of their prey. Although my experimental design (small spatial scale) would inevitably underestimate the movement cost of predators, this is the first study to experimentally demonstrate the importance of the relative timing (not the absolute timing) of prey phenology between local habitats in determining a prey-predator interaction in spatially structured environments.

Phenological tracking by predator and prey survival

While it has become evident that consumers can extend their foraging opportunities by tracking spatial variations in phenology of their resource species (Schindler *et al.* 2013), no studies have empirically tested how this phenological tracking by consumers can affect survival of resource species and hence their population dynamics on local and regional scale. In this study, I found that newts in asynchronous treatments spent more time in tanks with higher density of tadpoles both in the early and late periods relative to newts in synchronous treatment, suggesting that the newts tracked spatial variations in prey phenology between local habitats. Consequently, the survival of tadpoles in local habitats was generally lower in asynchronous relative to synchronous treatments in both periods. The significant negative relationship between the residence time of newts and the survival of tadpoles supports the inference that the movement patterns of the newt can directly affect survival of tadpoles on the local scale. However,

this relationship was stronger in the early period than the late period. There are two possibilities explaining the inconsistency between the two periods. First, the starvation of the newts might increase their predation pressure on tadpoles in the late-synchronous treatment, thereby depressing the effect of synchrony. However, I think this explanation is unlikely because the differences in tadpole survival between treatments with predator presence (E_{P+}/L_{P+}) and absence (E_{P-}/L_{P-}) were similar between the early and late periods. Second, the natural mortality of tadpoles was higher in the late period than the early period, which might mask the benefit of the phenological synchrony. Because I used tadpoles from multiple females (> 20 females) in each period, the lower mortality in the late period did not result from a sampling of females with low egg qualities. Alternatively, relatively high water temperature during the late period might negatively affect tadpole survival during their early developmental stage (Smith-Gill & Berven 1979). This scenario is speculative at present; however, it would be worth testing whether the benefits of reproductive synchrony depend on the absolute timing that should be determined by the physiological cost and benefit of the spawning timing.

Theory predicts that when prey in spatially heterogeneous environments are vulnerable to mobile predators only in their early developmental stage, total survival of prey among populations should be higher in spatially synchronous populations than in asynchronous populations (i.e., EE/LL > EL in this study) (Ims 1990a). Contrary to this theoretical prediction, the total survival of tadpoles was higher in treatments with the late tadpole addition at the end of the late period (i.e., EE < EL < LL), but no significant treatment effect was found 23-days after the end of the late period. This inconsistency with the theory might be because tadpoles were vulnerable to predation by newts throughout the experiment (i.e., prey was not ephemeral resource for newts) due to their limited growth rate (Online resource 2), and it would mask the positive effect of

synchrony. Specifically, most of the tadpoles in the experiment were not big enough to reach size refuge of the newt predation even at the end of the experiment (K. Takahashi, personal observation). Hence, although I thought that the total survival was better to be evaluated by the number of metamorphosing tadpoles in each enclosure, instead of the number of tadpoles counted at arbitrary defined timing, I found only a few metamorphosed individuals across all treatments. This would be because the productivity (nutrient concentration, GPP and periphyton biomass) of tanks was generally low throughout the experiment (Online resource 2). Although these results could be an artifact of my experimental setting, my study implies that the effects of phenological synchrony depends on habitat productivity that affects growth rate of prey and hence regulates the duration at which prey are vulnerable to predation.

Spatial scale of the experiment and potential factors affecting movement patterns of predator

In this study, I tested my hypothesis on relatively small spatial scale, which is liable to underestimate the movement cost of predator. Spatial scale and relevant prey-predator dynamics is continuous, and it is not easy to define the appropriate spatial scale for empirical studies. Despite this limitation, I would argue that the two-patch habitat will be qualitatively different with a single habitat with the same total habitat area. My experimental design allowed me to demonstrate that the phenological variation between local habitats and its tracking by predator would be a key to determine prey-predator interactions in spatially structured environments. Given the recent recognition of phenological variations on small spatial scale, the spatially structured prey-predator dynamics would be rather common than previously expected (Armstrong *et al.* 2016). However, my results should be understood with caution in the spatial context because

distances among local habitats will certainly affect the movement costs of predators. A next step of the empirical works is to clarify the influence of preys' phenological synchrony on their survival under different costs of predators' movement patterns. In this study, I tested my hypothesis on relatively small spatial scale, which is liable to underestimate the movement cost of predator. Spatial scale and relevant prey-predator dynamics is continuous, and it is not easy to define the appropriate spatial scale for empirical studies. Despite this limitation, I would argue that the two-patch habitat will be qualitatively different from a single habitat with the same total habitat area. My experimental design allowed me to demonstrate that the phenological variation between local habitats and phenological tracking by predator would be a key to determine prey-predator interactions in spatially structured environments. Given the recent recognition of phenological variations on small spatial scale, the spatially structured prey-predator dynamics would be rather common than previously expected (Armstrong *et al.* 2016). However, my results should be understood with caution in the spatial context because distances among local habitats will certainly affect the movement costs of predators. A next step of the empirical works is to clarify the influence of preys' phenological synchrony on their survival under different costs of predators' movement patterns.

Theoretically, movement patterns of predators have been predicted to be important in the evolution of reproductive synchrony in prey (Ims 1990b), as well as community dynamics (McCann *et al.* 2005; Kondoh *et al.* 2016), in spatially structured environments. These theories have assumed that predators move freely among habitats, depending on the spatial variation in prey densities. This is a conceiving assumption satisfying the principle of adaptive foraging theory, in which predators should behave to maximize the efficiency of their energy gain (Bedoya-Perez *et al.* 2013). In my study, newts stayed significantly longer times in tanks with more tadpoles than the tanks with

no or less tadpoles in an asynchronous treatment, supporting the density-dependent movement pattern. On the other hand, I found individual variation in movement patterns of newt in the synchronous treatment, and this variation explained the variation in survival of tadpoles between the two tanks in an enclosure. Although I could not identify the causes of the movement patterns of newts in this study, it generally depends on multiple interacting factors including movement costs (Russell *et al.* 2003), trait variation among individuals (Nifong *et al.* 2014) and spatial memory (Merkle *et al.* 2014). Elucidating these complex decision-making processes would improve predictions of spatially structured prey-predator interactions with realistic assumptions of the trade-off between movement costs and energy gain.

Conclusion

While many studies have highlighted the important role of temporal variation in phenology plays in determining prey-predator interactions within a single habitat, I argue that spatial variation in phenology appears to play an important role similarly in spatially structured environments. Given a general trend of higher mobility of organisms at higher trophic positions (e.g., predator couples patchy habitats of prey) (Rooney *et al.* 2008), this argument would be broadly applicable to understand other species interactions, such as plant-herbivore and plant pollinator interactions. However, at this point, I cannot gain insights beyond the fact that spatial variation in resource phenology can affect their survival through the phenological tracking by consumers. Future studies will be essential to clarify the mechanisms of individual variation in movement patterns, which will advance my understanding of species interactions in spatially structured environments. Furthermore, revealing physiological mechanisms of prey phenology and its relative importance to predation will be necessary to answer a fundamental question why

phenology of prey vary in time and space. Integrating these studies will allow us to develop a general framework to better predict the effects of spatiotemporal variations in phenology on species interactions in heterogeneous environments.

Chapter 4
Spatiotemporal variation in phenology affects metapopulation dynamics

Introduction

Because the timing of life-history events is a crucial factor determining individual fitness, the relationship between phenology and population dynamics has been well-studied (Post & Forchhammer 2002). In particular, the match-mismatch hypothesis predicts an increase in prey abundance when vulnerable life-stages do not overlap with the seasonal increase in predation pressure (Durant *et al.* 2007). However, most previous studies were conducted in a single habitat (but see Ims 1990b). Few studies have considered the relationship between phenology and population dynamics in spatially structured habitats, in which individuals can forage or disperse within a generation. In spatially structured habitats, phenology can vary spatially among habitats because of the differential effects of the environmental factors and potential demographic stochasticity among habitats (Chapter 2). Spatial variation in prey phenology and predator movements in spatially structured habitats cause unique ecological phenomena, such as phenological tracking by predators (Deacy *et al.* 2016). As shown in Chapter 3, such phenological tracking can strongly regulate the survival rate of prey in a certain habitat, suggesting that absolute phenology (i.e., calendrer date) but relative phenology with neighboring habitats (i.e., degree of synchrony) can be a critical component determining prey-predator interactions in the spatially structured habitat (Takahashi & Sato 2017).

Annual shifts of spatial variation in phenology are also important for metapopulation dynamics on a small spatial scale. As described in Chapter 2, demographic stochasticity might influence phenological variation both spatially and

annually. Demographic stochasticity predicts that annual variation in small population tends to be large. Therefore, metapopulation dynamics with demographic stochasticity in phenology would depend on the sizes of local populations. Conversely, spatial variation caused by environmental fluctuation might shift independent of local population size.

Dispersal is a driving factor of population dynamics in spatially structured habitats, which is known as a "metapopulation". For example, a mathematical model predicted that metapopulation dynamics can be stabilized when the dispersal rate is high (Gyllenberg *et al.* 1993). The "Two-population metapopulation model", in which the effects of dispersal between two local populations are considered, is a classical and simple metapopulation model (Hanski 1999). This model can be extended to the matrix model to consider more realistic situations, in which the local population consists of multiple demographic classifications, such as life stage (Caswell 2001). Therefore, it is suitable for analyzing the population dynamics of animals with complex life cycles, such as amphibians (Schmidt *et al.* 2012).

The purpose of this study was to test whether spatial and annual variation in phenology can regulate metapopulation dynamics. To this end, matrix projection models were constructed to calculate the metapopulation dynamics of *Rhacophorus arborous* with spatial and annual variation in breeding phenology. I considered two metapopulation models, in which either habitat environment or demographic stochasticity was assumed as a driving factor of spatial variation. Although, these models are specialized to describe the metapopulation dynamics of *R. arboreus* in AFRS, this was the first study to test the effects of spatial and temporal variation in phenology on the metapopulation dynamics, which is of general interest in ecology.

Materials and methods

Environment model

The model describes the dynamics of two local populations, 1 and 2. I consider a local population to be stage-structured with three stages: juvenile, subadult, and adult. This three-stage formulation is employed because *R. arboreus* females mature at 3-years-old, on average (Maeda & Matsui 1999). I used a column vector $N(t)$ to denote the abundance of individuals at each stage for populations 1 and 2:

$$N(t) = \begin{pmatrix} J_1(t) \\ S_1(t) \\ A_1(t) \\ J_2(t) \\ S_2(t) \\ A_2(t) \end{pmatrix},$$

where, $J_i(t)$, $S_i(t)$, and $A_i(t)$ are the abundances of juveniles, subadults, and adults, respectively, in the local population i just before the breeding season of year t. At this point, juveniles have already metamorphosed and become froglets. Annual changes of $N(t)$ are described using a 6×6 projection matrix P composed of four submatrices:

$$P = \begin{pmatrix} L_1 & M_{2\to1} \\ M_{1\to2} & L_2 \end{pmatrix},$$

where, L_i is a 3×3 Leslie matrix defining birth, death, and stage transition in the local population i, and $M_{i\to j}$ is a 3×3 matrix describing movements of individuals from population i to j.

The Leslie matrix for population i is defined as

$$L_i = \begin{pmatrix} 0 & 0 & (1-e_{ji})F_{3i} \\ s_{21i} & 0 & 0 \\ 0 & s_{32i} & s_{33i} \end{pmatrix},$$

where, F_{3i} is the per capita production rate of juvenile by adults, s_{21i} is the survival (i.e., transition) rate from juvenile to subadults, s_{33i} is the survival (transition) rate from subadults to adults, s_{33i} is the survival rate of adults, and e_{ji} is the emigration

rate from population i to j.

Negative density dependence of the Beverton-Holt type is considered to regulate juvenile production by adults. The production rate for population i is defined as

$$F_{3\mathrm{i}} = f(\tau_i(t)) \left(\frac{1}{1+K_i^{-1} hCA(t)} \right) hC,$$

where, $f(\tau_i(\mathrm{t}))$ is the survival rate of juveniles determined by the breeding phenology of their adults in year t, K_i controls the strength of negative density dependence in juvenile production, and is independent of the breeding phenology of their adults, h is the egg hatching rate, and C is the clutch size of a single female (Kusano *et al.* 2005). Here, larger K_i alleviates negative density dependence and may represent a large pond and/or a pond environment suitable for tadpole survival. In this study, K_i is assumed to be a parameter of habitat size of the pond. The density of amphibians strongly affects individual fitness directly through tadpole survival and indirectly through post-metamorphosis survival depending on body size and seasonal timing at metamorphosis (Earl & Whiteman 2015). Negative density dependence in the juvenile stage is considered to capture all of these factors. To constrain the overall strength of negative density dependence across the two local populations, I set K_1+K_2 as a constant parameter. This setting is interpreted as the total habitat-size capacity for juvenile stages constant across the whole metapopulation, such that a larger K_1 (or K_2) is compensated by a smaller K_2 (or K_1).

The survival rate of juveniles depending on the breeding phenology of their adults modeled as:

$$f(\tau_i(\mathrm{t})) = \alpha \exp(-\beta \tau_i(\mathrm{t})^2),$$

where, $\tau_i(\mathrm{t})$ is a phenological peak of population i in year t, α is the maximum survival rate of juveniles when the breeding phenology of their adults is optimal (i.e., $\tau_i(\mathrm{t}) = 0$), and β determines the rate at which survival rates decline as the

breeding phenology departs from the optimal value. The unimodal shape of this survival function may be justified by the following reasons. First, the predation pressure of newts decreases as a breeding season advances, because newt density in ponds drops in summer in AFRS (Fig. 18). Second, with a delayed breeding season, tadpoles become more likely to experience high water temperature, and suffer from higher natural mortality (Chapter 3). Phenological peaks of population i in year t are assumed to follow a Gaussian distribution with mean $\tau_{mean,i}$ and standard deviation $\tau_{SD,i}$:

$$\tau_i(\mathrm{t}) \sim \mathrm{Gaussian}\left(\tau_{mean,i}, \tau_{SD,i}\right).$$

All survival and transition rates between stage classes are set to the same value m:

$$s_{21i} = s_{32i} = s_{33i} = m,$$

This assumption may be justified because subadults and adults occur on land at low densities and their survival rate does not seem to be regulated by any density-dependent processes (Kusano 1998). As the approximate lifetime of *R. arboreus* at 2–3 years is known from skeletochronological assessment (T. Kusano, personal communication), the value of m was calculated as an inverse of this lifespan.

Between-population dispersal is assumed to occur during the juvenile stage. Amphibians, including *R. arboreus*, present extreme site loyalty (Smith & Green 2005; Toda 2014). Therefore, a low rate of natal dispersal was assumed following metamorphosis in the juvenile stage. Migrant death was not considered in this study because froglets would usually move onto land for foraging and differences in the mortality rate between migrants and residents seems to be negligible. With the above formulae, the following equation describes the population dynamics of the metapopulation:

$$\begin{pmatrix} \mathrm{J}_1(\mathrm{t}+1) \\ \mathrm{S}_1(\mathrm{t}+1) \\ \mathrm{A}_1(\mathrm{t}+1) \\ \mathrm{J}_2(\mathrm{t}+1) \\ \mathrm{S}_2(\mathrm{t}+1) \\ \mathrm{A}_2(\mathrm{t}+1) \end{pmatrix} =$$

$$\begin{pmatrix} 0 & 0 & (1-e_{21})f(\tau_i(\mathrm{t}))\left(\frac{1}{1+\gamma_1 hCA(t)}\right)h_i N & 0 & 0 & e_{12}f(\tau_i(\mathrm{t}))\left(\frac{1}{1+\gamma_2 hCA(t)}\right)h_i N \\ m & 0 & 0 & 0 & 0 & 0 \\ 0 & m & m & 0 & 0 & 0 \\ 0 & 0 & e_{21}f(\tau_i(\mathrm{t}))\left(\frac{1}{1+\gamma_1 hCA(t)}\right)h_i N & 0 & 0 & (1-e_{12})f(\tau_i(\mathrm{t}))\left(\frac{1}{1+\gamma_2 hCA(t)}\right)h_i N \\ 0 & 0 & 0 & m & 0 & 0 \\ 0 & 0 & 0 & 0 & m & m \end{pmatrix}$$

$$\times \begin{pmatrix} \mathrm{J}_1(\mathrm{t}) \\ \mathrm{S}_1(\mathrm{t}) \\ \mathrm{A}_1(\mathrm{t}) \\ \mathrm{J}_2(\mathrm{t}) \\ \mathrm{S}_2(\mathrm{t}) \\ \mathrm{A}_2(\mathrm{t}) \end{pmatrix}.$$

Demographic stochasticity model

I considered demographic stochasticity in phenology in the two-population matrix model. To this end, the breeding phenology of each adult individual l in the whole study area is formulated as follows:

$$\mathrm{T}_l(\mathrm{t}) \sim \mathrm{Gaussian}(\mathrm{T}_{mean}, \mathrm{T}_{SD}),$$

where, $\mathrm{T}_l(\mathrm{t})$ is a normally distributed random variable with mean T_{mean} and standard deviation T_{SD}. Notes that $\mathrm{T}_l(\mathrm{t})$ represents individual phenology and is different from $\tau_i(\mathrm{t})$ in the environment model, which represents a phenological peak in population i in the year t. The survival rate of juveniles depends on the breeding phenology of adult l:

$$f(\mathrm{T}_l(\mathrm{t})) = \alpha \exp(-\beta \mathrm{T}_l(\mathrm{t})^2),$$

where, α is the maximum survival rate of juveniles when the breeding phenology of their

adults is optimal (i.e., $T_l(t) = 0$), and β determines the rate at which survival decline as the breeding phenology departs from the optimal value. Survival rate in population i is calculated by the mean of $f(T_l(t))$ and defined as:

$$g(T_l(t), A_i(t)) = \frac{\sum_l^{A_i(t)} f(T_l(t))}{A_i(t)}.$$

Finally, the per capita production rate of juveniles by adults in population i is described as:

$$F_{3i} = g(T_l(t), A_i(t)) \left(\frac{1}{1+K_i^{-1} hCA(t)}\right) hC.$$

Other equations in the Leslie matrix are the same as in the environment model. The projection matrix is described as the environment model.

Model Analysis

The dynamics of each population across 10,000 generations in the environment model and 30,000 generations in the demographic stochasticity models are calculated. The CV of the metapopulation was used as an index of population stability, and obtained by dividing the standard deviation of two populations in one generation by their sum. The first 10% of generations was not used because the dynamics of those generations is often dependent on the initial values. All statistical analyses were conducted in R v3.51 (Team & R Development Core Team 2016).

Results & Discussion

Metapopulation stability depended largely on the spatial and annual variation in phenology in the environment model. Specifically, metapopulation dynamics were stabilized when the annual mean phenological peaks ($\tau_{mean,i}$) in both populations approached the time when survival rate was maximal (Fig. 19a). Metapopulation

dynamics were also stabilized when the annual variation of phenological peaks ($\tau_{SD,i}$) in both populations was low (Fig. 19b). This would be because each population was stabilized when its annual variation in peak phenology was stable. The effects of phenology of each population on metapopulation stability depended on the habitat size of ponds (K_i). As the habitat size of a certain population increases, the effects of the mean and annual variance of phenological peaks on metapopulation stability increase (Fig. 19c, d).

The importance of dispersal for metapopulation stability depended on annual variation in the phenological peak ($\tau_{SD,i}$). Specifically, the dispersal rate did not affect metapopulation stability when $\tau_{SD,i}$ was low (approximately $\tau_{SD,i} < 1$, Fig. 20a). However, the higher dispersal rate resulted in a more stable metapopulation when $\tau_{SD,i}$ was high (Fig. 20b). This was likely due to immigrants from a donor population helping to maintain the recipient population size by increasing the dispersal rate, especially when the population dynamics became unstable due to the large fluctuations in the phenological peaks (i.e., high $\tau_{SD,i}$). Conversely, immigrants did not positively affect the recipient population size, because local population dynamics were relatively stable around the maximum population size when $\tau_{SD,i}$ was low. In this case, emigration that decreased the donor population size would negatively affect the metapopulation size and hence stability over time. These processes would be apparent when the donor population was large, and the recipient population was small. Immigration from a large, donor population can increase the abundance of a small, recipient population, resulting in stabilization of metapopulation dynamics even with a low immigration rate.

In the demographic stochasticity model, the dynamics of each population were dependent on its habitat size. The dynamics of the large habitat were stabilized and the dynamics of the other small habitat were destabilized as predicted by the demographic

stochasticity process. However, contrary to the environment model, metapopulation dynamics were independent of local habitat sizes in the broad ranges of the parameter setting, which represent the mean value and the annual variance of phenological peaks over the whole study site ($T_{mean,i}$ and $T_{SD,i}$; Fig. 21). This is likely because stabilization in the large population is counteracted by the small population in the metapopulation dynamics. In this model, the total habitat-size capacity for juvenile stages in the metapopulation was constant. Therefore, as the habitat size of a certain population increased, and its population dynamics stabilized by demographic stochasticity, the habitat size of the other population decreased and destabilized.

Dynamics of the metapopulation in the demographic stochasticity model were dependent on the migration rate. When habitat sizes between the two populations are equal, metapopulation dynamics were stabilized if the two populations had an equal immigration rate (Fig. 22a). Conversely, when the habitat sizes differed between the two populations, the metapopulation stability was maximized under the following two conditions: (1) the emigration rate from a small population was high and (2) the emigration rate from a large population was low (Fig. 22b). In other words, metapopulation dynamics could be stabilized when the two populations exchanged the same number (not ratio) of migrants. The following processes explain this. First, emigrants did not increase the recipient population and decreased the donor population in the demographic stochasticity model, because the dynamics of both local populations were relatively stable around the maximum population size, as denoted in environment model with low $\tau_{SD,i}$. Therefore, the sum of the local populations (i.e., metapopulation abundance) was maximized when two population exchanged an equal number of migrants. Second, as their population sizes increase, the dynamics of each population stabilize because of demographic stochasticity. Although both the abundance (i.e., mean) and its

standard deviation of the metapopulation were also critical determinants for the stability of metapopulation dynamics (i.e., CV), the standard deviation resulting from demographic stochasticity contributed more to stabilization than mean abundance. Specifically, the abundance ranged from 48.03 to 48.30 while the standard deviation of the metapopulation ranged from 2.91 to 3.06 when the habitat sizes were equal between the two populations.

In this study, I provided simple matrix models that consider spatiotemporal variation in phenology. These models can easily incorporate some important parameters, which could be estimated from field surveys. Specifically, while I arbitrarily assume the phenological peak $[\tau_i(t)]$ in the environment model, the model can set the phenological peak for each population, which was obtained as the median phenology in Chapter 2. By using the field data set across several years, the $\tau_{mean,i}$ and $\tau_{SD,i}$ in each population can be estimated. Relative habitat sizes (ratio of K_1 and K_2) can also be obtained by the number of foam nests in each site as well. It is possible that the relative population size of each site in AFRS did not vary considerably because the numbers of foam nests were positively correlated over 5 years (Chapter 2). The models revealed that the dispersal rate between local populations affected metapopulation dynamics. Genome-wide single nucleotide polymorphisms detection, by RAD-seq and MIG-seq, is useful for estimating the dispersal rate per generation, which will be directly applicable to the model (Suyama & Matsuki 2015; Grummer & Leaché 2017). By adopting those parameters, filled data-driven models can be constructed, enabling us to make predictions for each ecological situation.

Habitat networks consisting of more than three habitats are known to influence metapopulation dynamics (Holyoak 2000; Fortuna *et al.* 2006). Although in this study, metapopulation models with only two local populations were analyzed, the models can

be easily extended to those having more than two populations. Spatial variations in phenology among local populations would be more complex in nature than assumed in these models. For example, altitude in mountainous area can cause directional spatial variation in phenology from the bottom to the top of the mountain (Schwartz 1998). Conversely, water temperature, which is determined by geomorphology (e.g., spatial variation in spring water) may show discrete spatial variation in phenology across landscape (Schindler *et al.* 2013). Demographic stochasticity in phenology also causes patchy spatial distribution. In the discrete distribution of phenology, the survival rate of migrants may depend on the distance and phenology of donor population. Further studies should test metapopulation dynamics considering spatially structured habitats using more explicitly and realistically developed models.

Previous studies have demonstrated that spatial variation in phenology on a relatively small spatial scale influences fitness components of organisms (e.g., Walter et al. 2015). Therefore, phenological variation through time and space might determine population dynamics in spatially structured habitats; however, this remains unknown. As dispersal among local populations is an important factor in such habitats, the metapopulation model is suitable to test the effects of spatial and temporal variation in phenology on the dynamics of spatial structured populations. The metapopulation models revealed that spatial and temporal variations in phenology are important for determining metapopulation stability over the broad range of the parameter setting. Interestingly, the phenology of a given local population is influential for its dynamics and for determining the importance of dispersal in stabilizing the dynamics of a metapopulation. Moreover, demographic stochasticity revealed that metapopulation stability depended on the balance of migration between populations, which was not found in the environment model. Considering that dispersal among local populations is common on a small spatial scale,

demographic stochasticity might influence metapopulation dynamics in spatially structured habitats. Moreover, these results suggest that it is important to identify the mechanisms underlying spatial and temporal variation in phenology to better understand population dynamics on a small spatial scale.

Chapter 5
General Discussion

Phenology has been an important factor mediating interspecific interactions and population dynamics in natural ecosystems. Its importance has increased to predict the effects of recent climate change on organisms. Although many studies have compared phenological variation among populations on a geographic scale and its ecological consequences, the causes and consequences of phenological variation on relatively small spatial scales remain unknown. On this scale, spatial variation may be caused by factors other than environmental factors (i.e., demographic stochasticity in phenology; see Chapter 2) and phenological tracking by organisms, which may lead to unique spatial interspecific interactions (see Chapter 3).

In this thesis, I examined annual and spatial variation in the breeding phenology of *Rhacophorus arboreus* on a small spatial scale (< 10 km^2) and demonstrated its consequence for prey-predator interactions and metapopulation stability. In Chapter 2, I estimated the annual and spatial variation in *R. arboreus* breeding phenology over 5 years, and stated that demographic stochasticity is a potential factor causing annual and spatial variation in the breeding phenology of *R. arboreus*. In Chapter 3, I showed that the observed spatial variation caused phenological tracking of the predator *Cynops pyrrhogaster*, which led to the survival rates of larval *R. arboreus* to be determined in a mesocosm experiment. In Chapter 4, I integrated field data into a mathematical model and suggested that spatial and temporal variation in *R. arboreus* breeding phenology affect their metapopulation dynamics. A key argument emerging from these results is that demographic stochasticity and environmental factors have different consequences for metapopulation stability, because the spatial and temporal variation in phenology had

larger effects on metapopulation stability.

Previous studies have examined spatial variation in phenology on a geographic scale mainly to explore environmental signals that determine the timing of life-history events. Conversely, phenological variation on a relatively small spatial scale has yet to be investigated, partly because environmental characteristics usually do not differ significantly among habitats on this spatial scale. However, as I have demonstrated in this thesis, demographic stochasticity may induce ecologically meaningful spatial variation in phenology, although the degree of demographic stochasticity might depend on other factors, such as environmental and/or genetic variations that are maintained in a certain region. Phenological variation on a small spatial scale may be more common than previously thought, because the demographic stochasticity in phenology would cause regardless of species and habitat environments only if populations consist of small sub-populations (e.g., Hanski *et al.* 1995). Furthermore, given that predators usually forage within a range that is broader than their preys' behavioral range (McCann *et al.* 2005), phenological tracking on a small spatial scale would be a common phenomenon (Armstrong *et al.* 2016). Since many studies have demonstrated that interspecific interactions caused by phenological matching can strongly determine individual fitness and population dynamics in a single habitat (Durant *et al.* 2007; Yang & Rudolf 2010), spatial variation in phenology is expected to further affect local/metapopulation dynamics in spatially structured habitats. To test this, I constructed a mathematical model that explicitly considers spatiotemporal variations in phenology, and demonstrated that metapopulation stability of *R. arboreus* was largely dependent on phenological variation in time and space. The models presented in this thesis are specific to the life history of *R. arboreus*. However, because both dispersal and differences in survival rate among habitats, caused by spatial variation in phenology, would be common in spatially

structured habitats on small spatial scales, the results showing that phenological variation regulates metapopulation dynamics might be applied to other organisms; however, further research is needed. Finally, the causes of this organisms' seasonal timings in life-history events have been of interest throughout human history at anytime and anywhere (Post & Inouye 2008). In conclusion, the moment has come to consider the causes and consequences of phenological variation through time and space to better understand the dynamics of organisms in nature.

Acknowledgements

First of all, I appreciate to T. Sato for his cordial support and encouragement throughout this thesis. I am grateful to H. Kawai, T. Mimura, A. Ushimaru, Y. Takami, S. M. Naman, T. Kusano and G. Takimoto for valuable comments and edits that improved the draft version of the manuscript. I thank M. Kanaiwa and K. Fukaya for advice on the data analysis. N. Tokuchi, T. Ise, M. Ishihara, K. Fukushima, H. Nakagawa, all staffs of AFRS and members of my laboratory are acknowledged for helping field and laboratory works.

This study was financially supported by grants from Kansai Organization for Nature Conservation in 2014, Fujiwara Natural History Foundation in 2017 and JSPS KAKENHI Grant Number 18J11294 in 2018.

References

Akaike, H. (1987). Factor analysis in AIC. *Psychometrika*, 52, 317–332.

Armstrong, J.B., Takimoto, G., Schindler, D.E., Hayes, M.M. & Kauffman, M.J. (2016). Resource waves: phenological diversity enhances foraging opportunities for mobile consumers. *Ecology*, 97, 1099–1112.

Bartlett, M.S. (1960). *Stochastic population models in ecology and epidemiology*. MethuenWiley.

Bedoya-Perez, M.A., Carthey, A.J.R., Mella, V.S.A., McArthur, C. & Banks, P.B. (2013). A practical guide to avoid giving up on giving-up densities. *Behav. Ecol. Sociobiol.*

Carle, F.L. & Strub, M.R. (1978). A new method for estimating population size from removal data. *Biometrics*, 34, 621.

Caswell, H. (2001). *Matrix population models: construction, analysis, and interpretation*. Updated ed. Oxford University Press.

Coogan, S.C.P., Nielsen, S.E. & Stenhouse, G.B. (2012). Spatial and temporal heterogeneity creates a “BrownTide” in root phenology and nutrition. *ISRN Ecol.*, 2012.

Deacy, W., Leacock, W., Armstrong, J. & Stanford, J.A. (2016). Kodiak brown bears surf the salmon red wave: Direct evidence from GPS collared individuals. *Ecology*, 97, 1091–1098.

Doi, H. & Takahashi, M. (2008). Latitudinal patterns in the phenological responses of leaf colouring and leaf fall to climate change in Japan. *Glob. Ecol. Biogeogr.*, 17, 556–561.

Durant, J.M., Hjermann, D.Ø., Ottersen, G. & Stenseth, N.C. (2007). Climate and the

match or mismatch between predator requirements and resource availability. *Clim. Res.*, 33, 271–283.

Earl, J.E. & Whiteman, H.H. (2015). Are commonly used fitness predictors accurate? A meta-analysis of amphibian size and age at metamorphosis. *Copeia*, 103, 297–309.

Engen, S., Bakke, O. & Islam, A. (1998). Demographic and environmental stochasticity-concepts and definitions. *Biometrics*, 54, 840–846.

Forrest, J. & Miller-Rushing, A.J. (2010). Toward a synthetic understanding of the role of phenology in ecology and evolution. *Philos. Trans. R. Soc. B Biol. Sci.*, 365, 3101–3112.

Fortuna, M.A., Gómez-Rodríguez, C. & Bascompte, J. (2006). Spatial network structure and amphibian persistence in stochastic environments. *Proc. R. Soc. B Biol. Sci.*, 273, 1429–1434.

Fox, J. & Weisberg, S. (2011). *An R companion to applied regression*. 2nd edn. SAGE Publication, Thousand Oaks.

Fréville, H., Colas, B., Riba, M., Caswell, H., Mignot, A., Imbert, E., *et al.* (2004). Spatial and temporal demographic variability in the endemic plant species *Centaurea corymbosa* (Asteraceae). *Ecology*, 85, 694–703.

Fryxell, J.M., Wilmshurst, J.F., Sinclair, A.R.E., Haydon, D.T., Holt, R.D. & Abrams, P.A. (2005). Landscape scale, heterogeneity, and the viability of Serengeti grazers. *Ecol. Lett.*, 8, 328–335.

Gosner, K.L. (1960). A simplified table for staging anuran embryos larvae with notes on identification. *Herpetologica*, 16, 183–190.

Grummer, J.A. & Leaché, A.D. (2017). Do dams also stop frogs? Assessing population connectivity of coastal tailed frogs (*Ascaphus truei*) in the North Cascades National Park Service Complex. *Conserv. Genet.*, 18, 439–451.

Gyllenberg, M., Söderbacka, G. & Ericsson, S. (1993). Does migration stabilize local population dynamics? Analysis of a discrete metapopulation model. *Math. Biosci.*, 118, 25–49.

Hanski, I. (1999). *Metapopulation ecology*. Oxford University Press, New York.

Hanski, I., Pakkala, T., Kuussaari, M. & Lei, G.L. (1995). Metapopulation persistence of an endangered bytterfly in a fragmented landscape. *Oikos*, 72, 21–28.

Holyoak, M. (2000). Habitat patch arrangement and metapopulation persistence of predators and prey. *Am. Nat.*, 156, 378–389.

Ims, R.A. (1990a). On the adaptive value of reproductive synchrony as a predator-swamping strategy. *Am. Nat.*, 136, 485–498.

Ims, R.A. (1990b). The ecology and evolution of reproductive synchrony. *Trends Ecol. Evol.*

Inouye, D.W. (2008). Effects of climate change on phenology, frost damage, and floral abundance of montane wildflowers. *Ecology*, 89, 353–362.

IPCC. (2007). *Climate Change 2007 Synthesis Report*. *IPCC*. Geneva, Switzerland.

Iwasawa, H. & Kawasaki, N. (1979). Normal stages of development of the japanese green frog *Rhacophorus arboreus* (Okada et Kawano). *Japanese J. Herpetol.*, 8, 22–35.

Kato, K. (1955). Ecological notes on the green frogs during the breeding season. I. *Japanese J. Ecol.*, 5, 70–73.

Kato, K. (1956). Ecological notes on the green frogs during the breeding season. II. *Japanese J. Ecol.*, 6, 57–61.

Koizumi, I. & Shimatani, I.K. (2016). Socially induced reproductive synchrony in a salmonid: an approximate Bayesian computation approach. *Behav. Ecol.*, 00, 1386–1396.

Kondoh, M., Mougi, A., Ushimaru, A. & Nakata, K. (2016). Adaptive movement and food-chain dynamics: towards food-web theory without birth–death processes. *Theor. Ecol.*, 9, 15–25.

Kusano, T. (1998). A radio-tracking study of postbreeding dispersal of the treefrog, *Rhacophorus arboreus* (Amphibia: Rhacophoridae). *Jpn. J. Herpetol*.

Kusano, T., Sakai, A. & Hatanaka, S. (2005). Natural egg mortality and clutch size of the Japanese treefrog, Rhacophorus arboreus (Amphibia: Rhacophoridae). *Curr. Herpetol.*, 24, 79–84.

Kusano, T., Sakai, A. & Hatanaka, S. (2006). Ecological functions of the foam nests of the Japanese treefrog, *Rhacophorus arboreus* (Amphibia, Rhacophoridae). *Herpetol. J.*, 16, 163–169.

Lane, S.J. & Mahony, M.J. (2002). Larval anurans with synchronous and asynchronous development periods: Contrasting responses to water reduction and predator presence. *J. Anim. Ecol.*, 71, 780–792.

Lawson, D.E. (1986). Response of permafrost terrain to disturbace: a synthesis of observations from northern Alaska, U.S.A. *Arct. Alp. Res.*, 18, 1–17.

Levin, S.A. (1992). The problem of pattern and scale in ecology: the Robert H. MacArthur award lecture. *Ecology*, 73, 1943–1967.

Lofsvold, D. (1988). Quantitative genetics of morphological differentiation in peromyscus. II. Analysis of selection and drift. *Evolution.*, 42, 54–67.

Maeda, N. & Matsui, M. (1999). *Frogs and Toads of Japan*. 2nd edn. Bun-Ichi Sogo Shuppan, Tokyo.

McCann, K., Rasmussen, J. & Umbanhowar, J. (2005). The dynamics of spatially coupled food webs. *Ecol. Lett.*, 8, 513–23.

Merkle, J.A., Fortin, D. & Morales, J.M. (2014). A memory-based foraging tactic

reveals an adaptive mechanism for restricted space use. *Ecol. Lett.*, 17, 924–931.

Moore, J.W. & Schindler, D.E. (2010). Spawning salmon and the phenology of emergence in stream insects. *Proc. R. Soc. B Biol. Sci.*, 277, 1695–1703.

Moran, P. (1953). The statistical analysis of the Canadian Lynx cycle. *Aust. J. Zool.*, 1, 291.

Nakazawa, T. & Doi, H. (2012). A perspective on match/mismatch of phenology in community contexts. *Oikos*, 121, 489–495.

Nifong, J.C., Layman, C.A. & Silliman, B.R. (2014). Size, sex and individual-level behaviour drive intrapopulation variation in cross-ecosystem foraging of a top-predator. *J. Anim. Ecol.*, 84, 35–48.

Post, E. (2003). Large-scale climate synchronizes the timing of flowering by multiple species. *Ecology*, 84, 277–281.

Post, E. & Forchhammer, M.C. (2002). Synchronization of animal population dynamics by large-scale climate. *Nature*, 420, 168–171.

Post, E. & Forchhammer, M.C. (2008). Climate change reduces reproductive success of an Arctic herbivore through trophic mismatch. *Philos. Trans. R. Soc. B Biol. Sci.*, 363, 2369–2375.

Post, E. & Inouye, D.W. (2008). Phenology: response, driver, and integrator. *Ecology*, 89, 319–320.

Post, E., Pedersen, C., Wilmers, C.C. & Forchhammer, M.C. (2008). Warming, plant phenology and the spatial dimension of trophic mismatch for large herbivores. *Proc. R. Soc. B Biol. Sci.*, 275, 2005–2013.

Rasmussen, N.L., Rudolf, V.H.W. & Cáceres, C.E. (2015). Phenological synchronization drives demographic rates of populations. *Ecology*, 96, 1754–1760.

Régnière, J. & Sharov, A. (1998). Phenology of *Lymantria dispar* (Lepidoptera:

Lymantriidae), male flight and the effect of moth dispersal in heterogeneous landscapes. *Int. J. Biometeorol.*, 41, 161–168.

Revilla, T.A., Encinas-Viso, F. & Loreau, M. (2014). (A bit) Earlier or later is always better: phenological shifts in consumer-resource interactions. *Theor. Ecol.*, 7, 149–162.

Rooney, N., McCann, K.S. & Moore, J.C. (2008). A landscape theory for food web architecture. *Ecol. Lett.*, 11, 867–881.

Ruff, C.P., Schindle, D.E., Armstrong, J.B., Bentle, K.T., Brooks, G.T., Holtgrieve, G.W., *et al.* (2011). Temperature-associated population diversity in salmon confers benefits to mobile consumers. *Ecology*, 92, 2073–2084.

Russell, R.E., Swihart, R.K. & Feng, Z. (2003). Population consequences of movement decisions in a patchy landscape. *Oikos*, 103, 142–152.

Sawyer, H. & Kauffman, M.J. (2011). Stopover ecology of a migratory ungulate. *J. Anim. Ecol.*, 80, 1078–1087.

Schindler, D.E., Armstrong, J.B., Bentley, K.T., Jankowski, K., Lisi, P.J. & Payne, L.X. (2013). Riding the crimson tide: mobile terrestrial consumers track phenological variation in spawning of an anadromous fish. *Biol. Lett.*, 9, 20130048.

Schmidt, B.R., Hodl, W. & Schaub, M. (2012). From metamorphosis to maturity in complex life cycles : equal performance of different juvenile life history pathways. *Ecology*, 93, 657–667.

Schneider, C.A., Rasband, W.S. & Eliceiri, K.W. (2012). NIH Image to ImageJ: 25 years of image analysis. *Nat. Methods*.

Schwartz, M.D. (1998). Green-wave phenology. *Nature*, 394, 839–840.

Smith-Gill, S.J. & Berven, K.A. (1979). Predicting amphibian metamorphosis. *Am. Nat.*, 113, 563–585.

Smith, M.A. & Green, D.M. (2005). Dispersal and the metapopulation in amphibian and paradigm ecology are all amphibian conservation: populations metapopulations ? *Ecography (Cop.).*, 28, 110–128.

Steinman, A.D., Lamberti, G.A. & Leavitt, P.R. (2006). Biomass and pigments of benthic algae. In: *Methods in Stream Ecology*, Methods in stream ecology (eds. Hauer, F.R. & Lamberti, G.A.). Academic Press, San Diego, CA, pp. 357–379.

Suyama, Y. & Matsuki, Y. (2015). MIG-seq: an effective PCR-based method for genome-wide single-nucleotide polymorphism genotyping using the next-generation sequencing platform. *Sci. Rep.*, 5, 12.

Takahashi, K. & Sato, T. (2015). Temporal and spatial variations in spawning of the forest green tree frog (*Rhacophorus arboreus*) in a mountainous area. *Herpetol. Notes*, 8, 395–400.

Takahashi, K. & Sato, T. (2017). Spatial variability in prey phenology determines predator movement patterns and prey survival. *Aquat. Ecol.*, 51, 377–388.

Team, R.D.C. & R Development Core Team, R. (2016). R: A Language and Environment for Statistical Computing. *R Found. Stat. Comput.*, 1, 409.

Toda, M. (2014). Conservation ecology of amphibians and reptiles, in relation to population dynamics: case studies on the green anole *Anolis carolinensis* and the treefrog *Rhacophorus arboreus*. Kanazawa University.

Uno, H. & Power, M.E. (2015). Mainstem-tributary linkages by mayfly migration help sustain salmonids in a warming river network. *Ecol. Lett.*, 18, 1012–1020.

Walter, J.A., Meixler, M.S., Mueller, T., Fagan, W.F., Tobin, P.C. & Haynes, K.J. (2015). How topography induces reproductive asynchrony and alters gypsy moth invasion dynamics. *J. Anim. Ecol.*, 84, 188–198.

Wells, K.D. (2007). *The Ecology and Behavior of Amphibians*. University of Chicago

Press, Chicago.

Wetzel, R. & Likens, G. (1991). *Limnological analyses*. Springer, Newyork.

van Wijk, R.E., Kölzsch, A., Kruckenberg, H., Ebbinge, B.S., Müskens, G.J.D.M. & Nolet, B.A. (2012). Individually tracked geese follow peaks of temperature acceleration during spring migration. *Oikos*, 121, 655–664.

Yang, L.H. & Rudolf, V.H.W. (2010). Phenology, ontogeny and the effects of climate change on the timing of species interactions. *Ecol. Lett.*, 13, 1–10.

Table 1. Physical characteristics of sites in the Ashiu Forest Research Station. Mean air temperature and mean depth in June 2018 are shown.

	Area (m^2)	Temperature (˚C)	Depth (mm)
Sites			
1	3.68	17.73	178
2	17.02	17.91	368
3	-	-	-
4	2.33	17.49	282
5	11.40	17.02	41
6	3.87	17.22	15
7	2.08	16.32	56
8	7.03	-	12
9	6.68	16.77	259
10	2.38	15.94	168
11	2.61	16.26	31
12	7.83	16.54	191
13	3.21	16.12	89
14	7.90	16.48	77
15	1.87	15.24	59
16	24.38	16.19	20
17	48.57	16.38	27
18	61.36	-	30
19	74.59	17.28	135
20	25.58	17.02	14
21	0.85	16.82	4
22	51.08	17.18	34
23	422.96	17.32	41

Table 2. Optimal generalized linear model (GLM) for the cumulative proportion of the total foam nests observed in each site. In the GLM analysis, site 1 and year (2014) were used as the contrast with the other sites and years.

		Value	Std. Error
Intercept		5.148	0.008
Year	2015	-0.003	0.006
	2016	-0.040	0.005
	2017	-0.017	0.005
	2018	-0.024	0.005
Sites	2	-0.008	0.010
	3	0.055	0.028
	4	-0.029	0.013
	5	0.003	0.016
	6	-0.017	0.036
	7	-0.048	0.014
	8	-0.021	0.011
	9	-0.011	0.011
	10	-0.027	0.017
	11	-0.033	0.016
	12	-0.043	0.010
	13	0.050	0.033
	14	-0.044	0.010
	15	-0.050	0.022
	16	-0.002	0.037
	17	-0.024	0.009
	18	-0.003	0.010
	19	-0.024	0.008
	20	0.030	0.013
	21	0.001	0.015
	22	-0.009	0.011
	23	0.015	0.009
Log (scale)		-2.642	0.015

Table 3. p-values for the randomization tests. An asterisk (*) denotes that phenology at population level is significantly later than the null hypothesis ($\alpha < 0.025$), while a dagger (†) denotes that phenology at population level is significantly earlier than the null hypothesis ($\alpha > 0.975$).

	2014	2015	2016	2017	2018
Sites					
1	0.000*	0.012*	0.769	0.095	0.839
2	0.000*	0.012*	0.929	0.014*	0.469
3	0.002	-	-	-	-
4	-	0.075	0.793	0.378	0.699
5	0.697	0.005*	0.007*	0.021*	0.478
6	0.303	-	-	0.04	-
7	0.915	0.811	0.777	0.676	0.817
8	0.632	0.012*	0.821	0.138	0.184
10	0.211	0.652	0.611	0.232	0.819
9	-	0.745	0.458	0.416	0.478
11	-	0.248	0.977†	0.154	0.609
12	0.643	0.784	0.991†	0.969	0.805
13	-	-	-	0.375	0.000*
14	0.727	0.822	0.067	0.108	0.337
15	-	0.144	0.912	0.814	-
16	0.156	-	-	-	-
17	0.018*	0.001*	0.968	0.001*	0.967
18	-	0.015*	0.515	0.269	0.017*
19	0.000*	0.974	0.875	0.999†	0.004*
20	-	-	0.001*	0.022*	0.295
21	-	-	0.098	0.001*	0.705
22	-	-	-	0.000*	0.46
23	-	-	0.000*	0.000*	0.002*

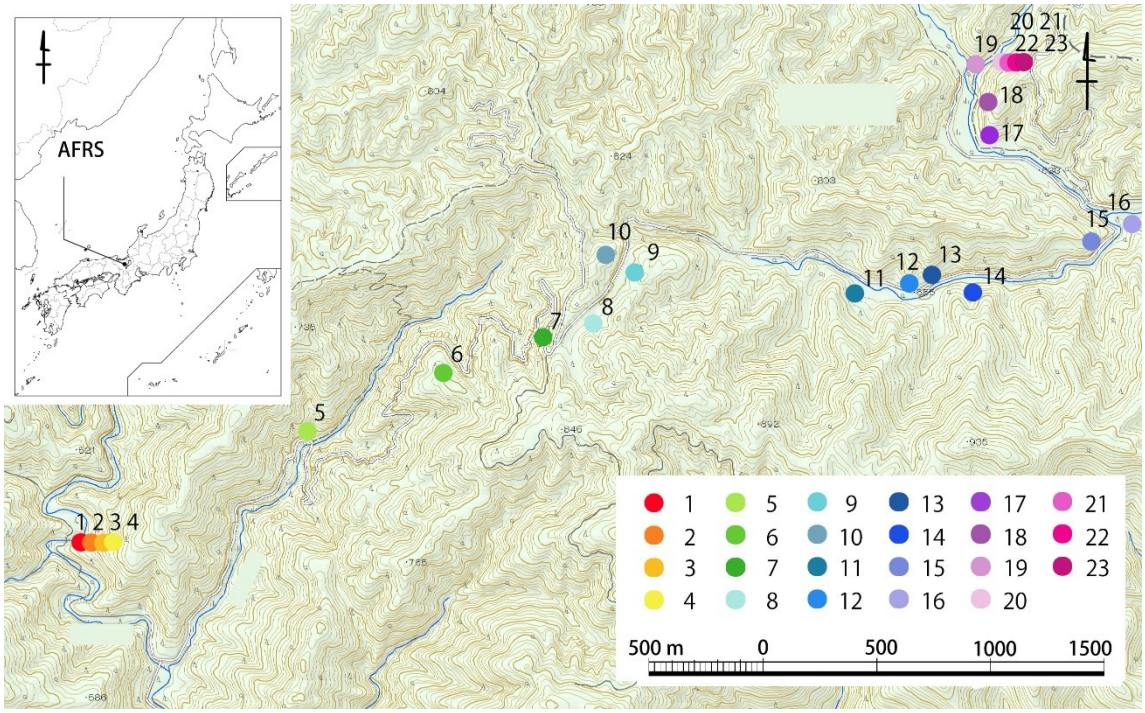

Fig. 1. Location of 23 sites in the Ashiu Forest Research Station (AFRS). Raw data for the location map were provided by the electronic contour map 25000 published by the Geospatial Information Authority of Japan.

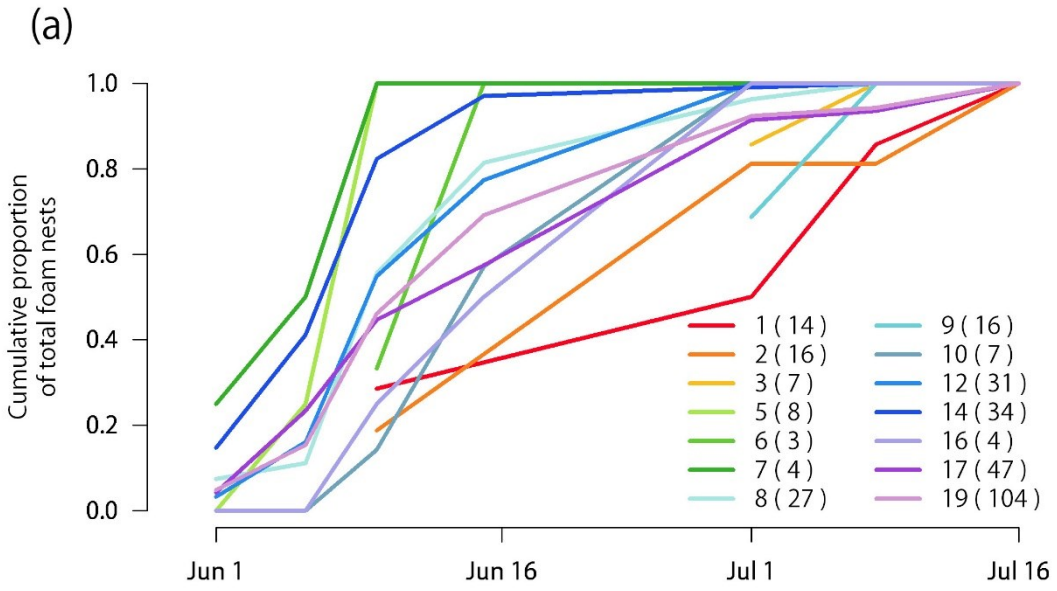
(a)
Cumulative proportion of total foam nests
1.0
0.8
0.6
0.4
0.2
0.0
Jun 1
Jun 16
Jul 1
Jul 16
1 (14)
2 (16)
3 (7)
5 (8)
6 (3)
7 (4)
8 (27)
9 (16)
10 (7)
12 (31)
14 (34)
16 (4)
17 (47)
19 (104)

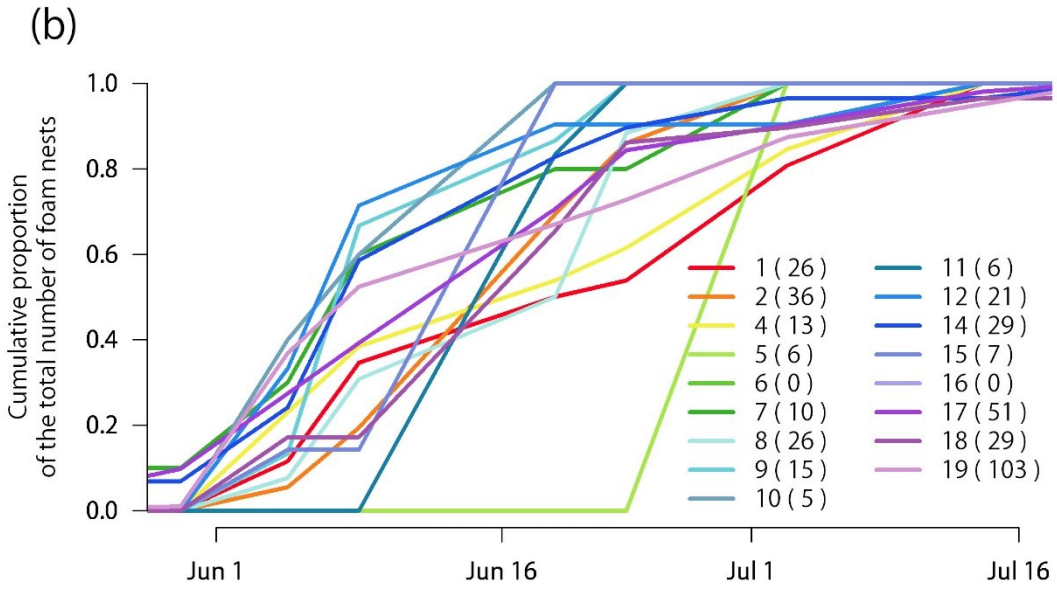
(b)
Cumulative proportion of the total number of foam nests
1.0
0.8
0.6
0.4
0.2
0.0
Jun 1
Jun 16
Jul 1
Jul 16
1 (26)
2 (36)
4 (13)
5 (6)
6 (0)
7 (10)
8 (26)
9 (15)
10 (5)
11 (6)
12 (21)
14 (29)
15 (7)
16 (0)
17 (51)
18 (29)
19 (103)

(c)

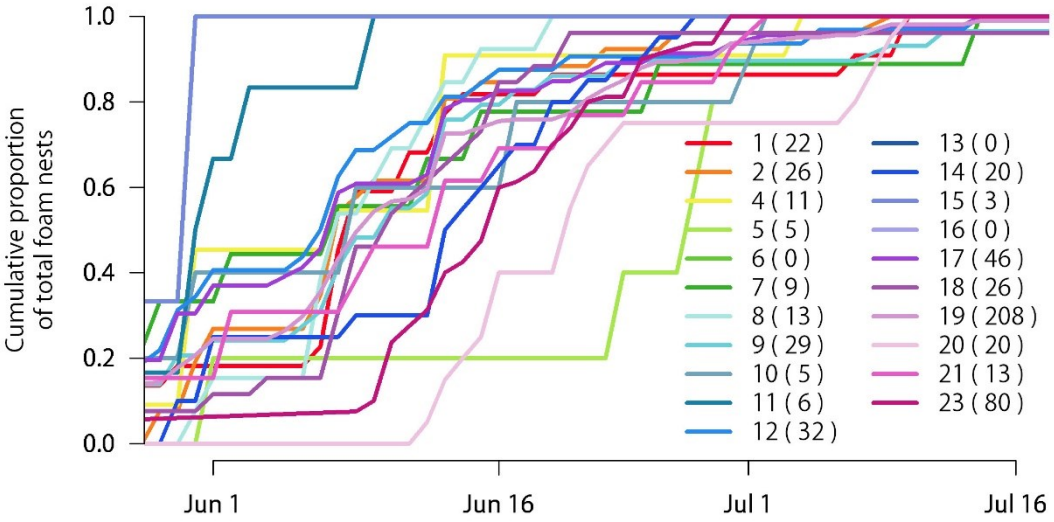
Cumulative proportion of total foam nests
1.0
0.8
0.6
0.4
0.2
0.0
Jun 1
Jun 16
Jul 1
Jul 16
1 (22)
2 (26)
4 (11)
5 (5)
6 (0)
7 (9)
8 (13)
9 (29)
10 (5)
11 (6)
12 (32)
13 (0)
14 (20)
15 (3)
16 (0)
17 (46)
18 (26)
19 (208)
20 (20)
21 (13)
23 (80)

(d)

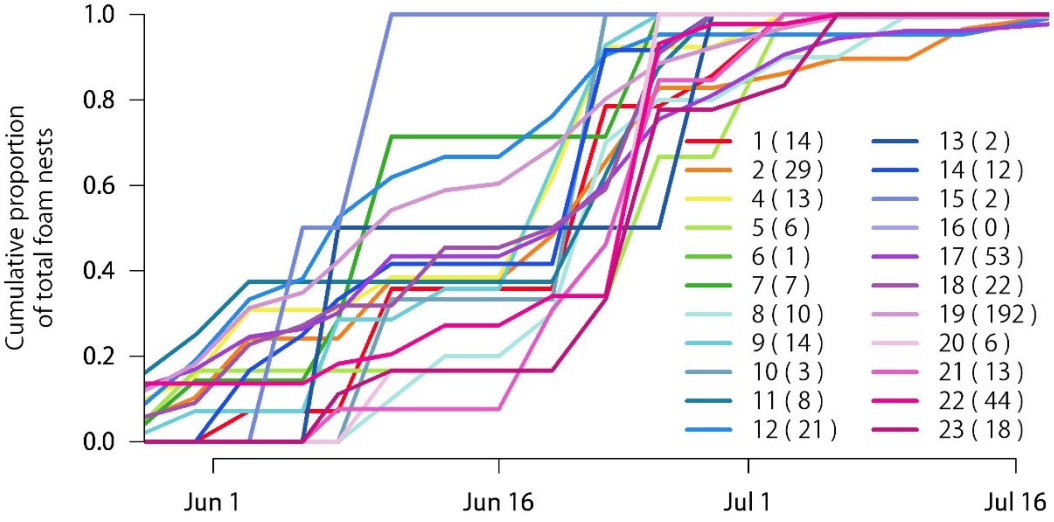
Cumulative proportion of total foam nests
1.0
0.8
0.6
0.4
0.2
0.0
Jun 1
Jun 16
Jul 1
Jul 16
1 (14)
2 (29)
4 (13)
5 (6)
6 (1)
7 (7)
8 (10)
9 (14)
10 (3)
11 (8)
12 (21)
13 (2)
14 (12)
15 (2)
16 (0)
17 (53)
18 (22)
19 (192)
20 (6)
21 (13)
22 (44)
23 (18)

(e)

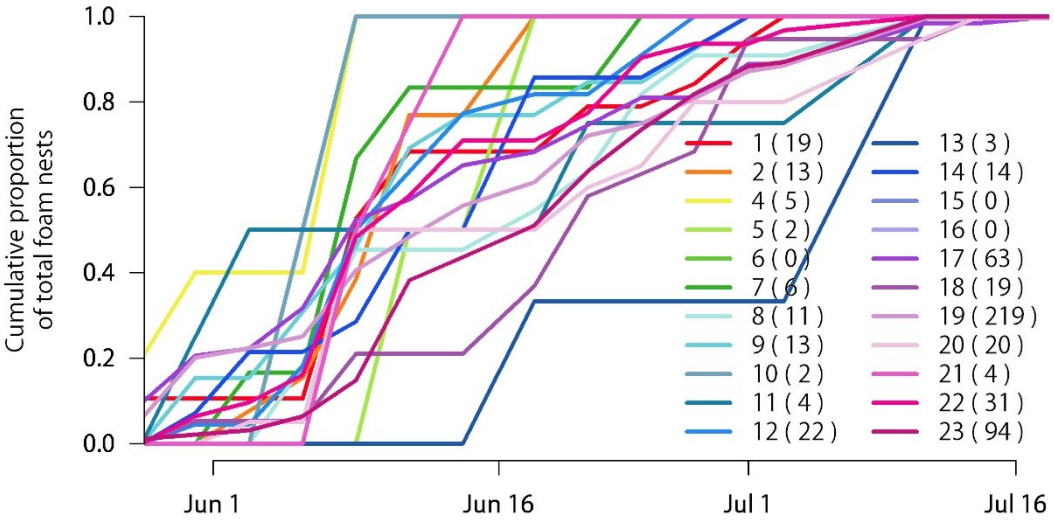
Cumulative proportion
of total foam nests
1.0
0.8
0.6
0.4
0.2
0.0
Jun 1
Jun 16
Jul 1
Jul 16
1 (19)
2 (13)
4 (5)
5 (2)
6 (0)
7 (6)
8 (11)
9 (13)
10 (2)
11 (4)
12 (22)
13 (3)
14 (14)
15 (0)
16 (0)
17 (63)
18 (19)
19 (219)
20 (20)
21 (4)
22 (31)
23 (94)

(c)

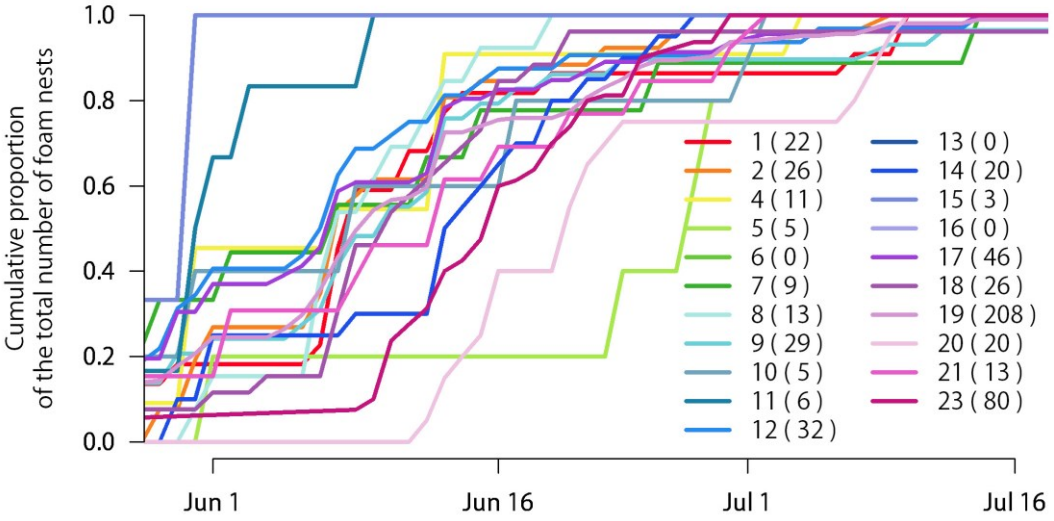
Cumulative proportion
of the total number of foam nests
1.0
0.8
0.6
0.4
0.2
0.0
Jun 1
Jun 16
Jul 1
Jul 16
1 (22)
2 (26)
4 (11)
5 (5)
6 (0)
7 (9)
8 (13)
9 (29)
10 (5)
11 (6)
12 (32)
13 (0)
14 (20)
15 (3)
16 (0)
17 (46)
18 (26)
19 (208)
20 (20)
21 (13)
23 (80)

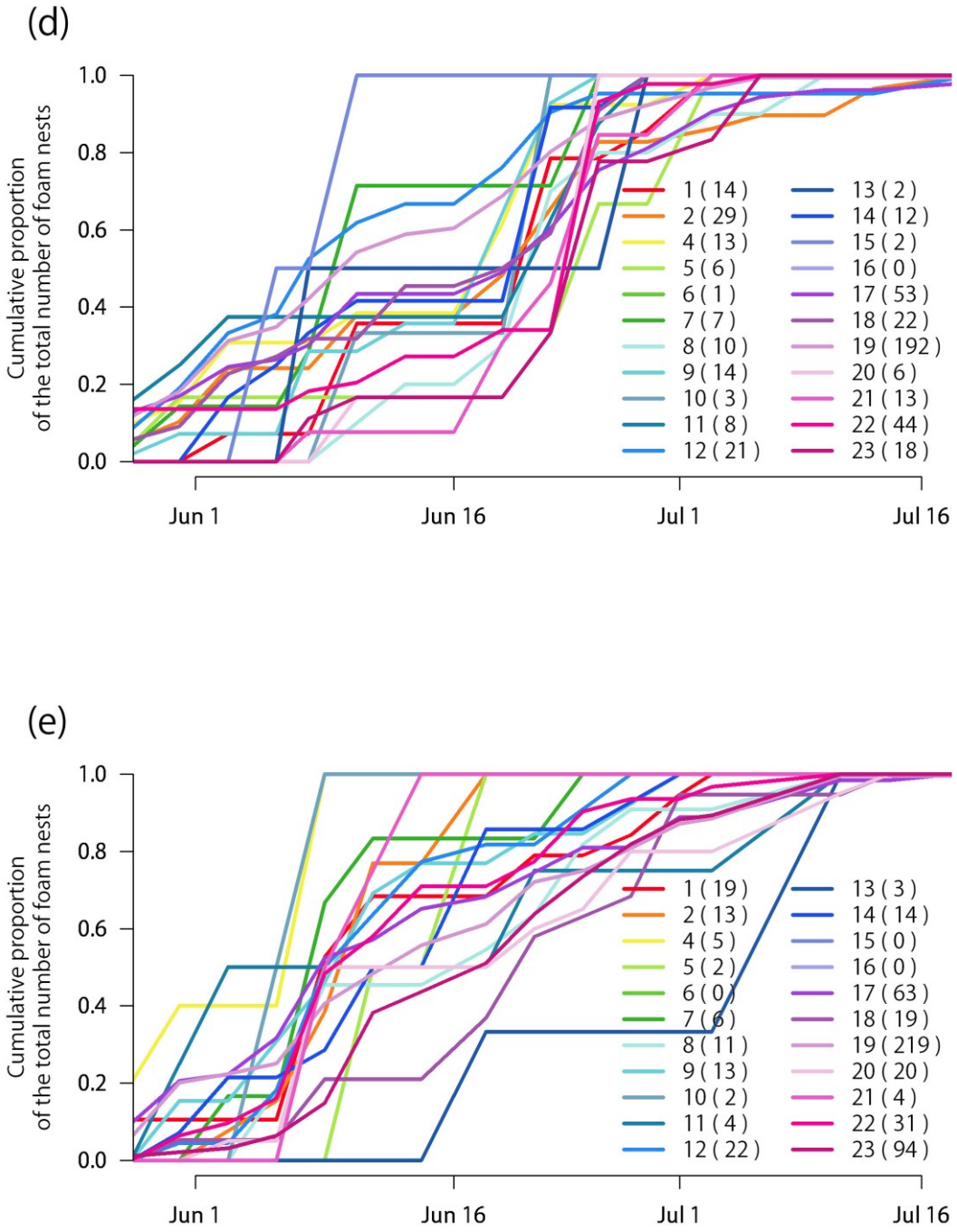

Fig. 2. Cumulative proportions of the total foam nests observed in each site during the field observation in (a) 2014, (b) 2015, (c) 2016, (d) 2017, and (e) 2018. Numbers in

parentheses represent the total numbers of foam nests observed in each site. Line colors correspond to those of the closed circles in Figure 1.

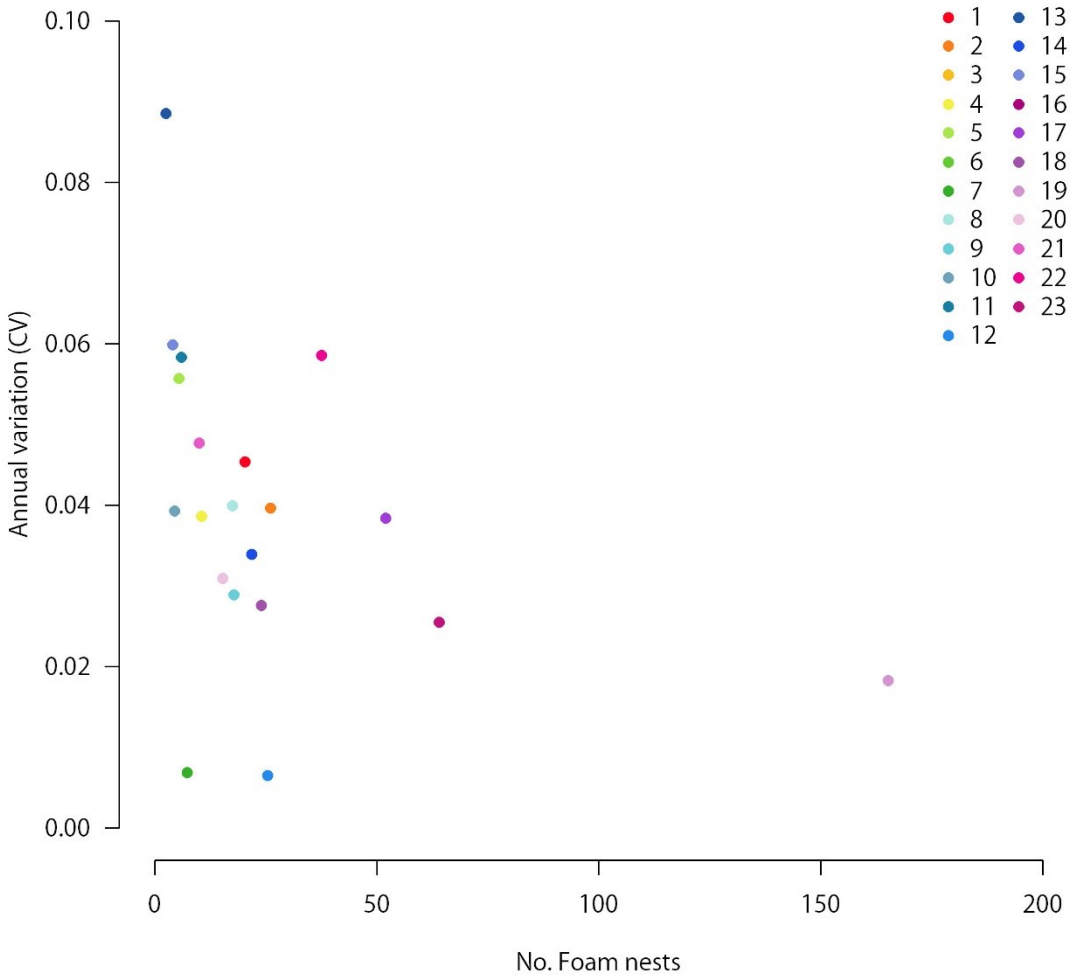

Fig. 3. Relationship between the mean number of foam nests over five years and annual variation in peaks of breeding phenology. Each circle denotes the median phenology at population level in each site and year. Each vertical bar represents annual variation in each site. Line colors correspond to the locations of the sites shown in Figure 1.

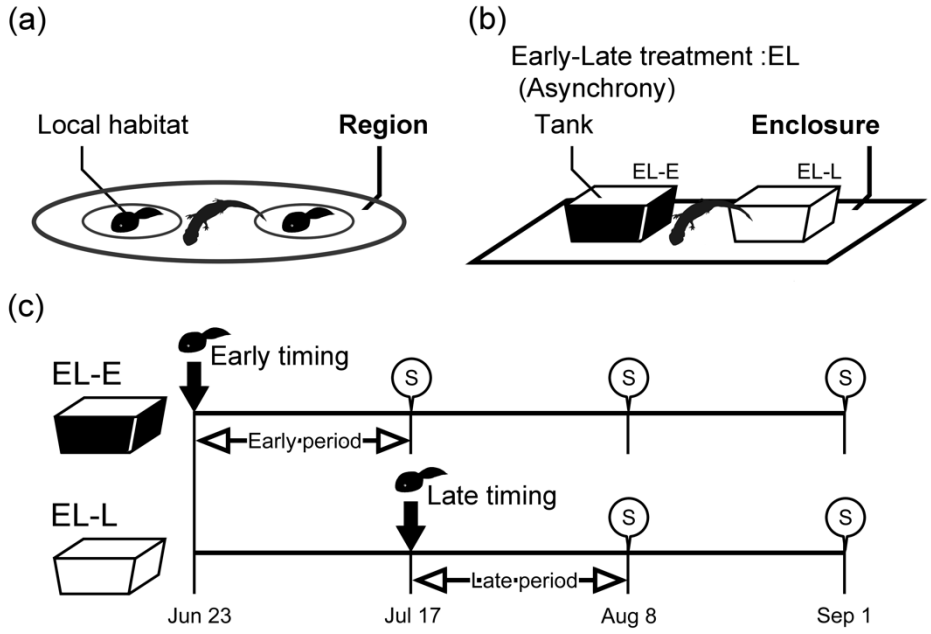

Fig. 4. A schematic diagram of the experiment. A spatially structured natural environment was shown in panel (a), while the experimental system that imitated the natural environment was represented in panel (b). The panel (c) shows the time schedule of the experiment. In the panel (b), tanks correspond to the local habitat and the enclosure does to the region in the natural environment. In the panel (c), EL-E and EL-L mean a tank in EL treatment that received tadpoles at the early timing and late timing, respectively. “S” in the panel (c) is a survey timing of the number of the tadpoles.

Fig. 5. Enclosures in the open field study site in Ashiu Forest Research Station of Field Science Education and Research Center, Kyoto University. During the experiment, all enclosures were covered by an 80%-shading net to simulate a natural habitat (light intensity: 1400-68800 lux during daytime). No other structures (e.g., canopy and/or building) that potentially affected light conditions of enclosures were present in the study site.

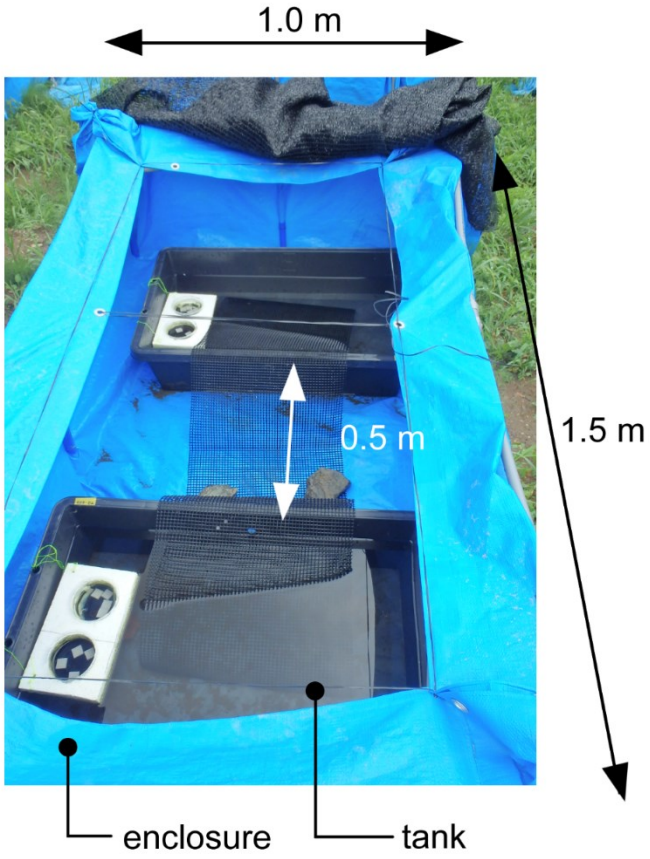

Fig. 6. Inside an enclosure with two tanks. The height of the enclosure was set at 0.5 m, which prevented the escapement of newts

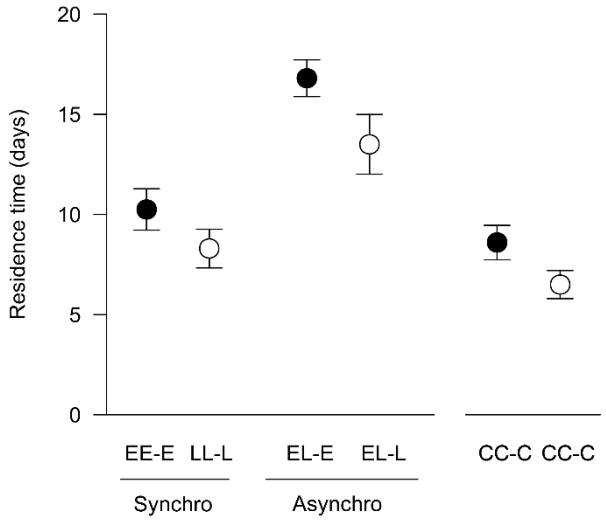

Fig. 7. The effects of treatments (synchrony/asynchrony/control) and periods (early/late) on the mean residence time (± SE) of newts in each tank. Solid circles denote the early period, while open circles represent the late period. There are four types of tanks across treatments: EE-E, a tank with tadpole addition at the beginning of the early period in a synchronous treatment (n = 20 tanks); LL-L, a tank with tadpole addition at the beginning of the late period in a synchronous treatment (n = 20); EL-E, a tank with tadpole addition at the beginning of the early period in an asynchronous treatment (n = 10); EL-L, a tank with tadpole addition at the beginning of the late period in an asynchronous treatment (n = 10). CC-C denotes a control tank with no tadpole addition (n = 20).

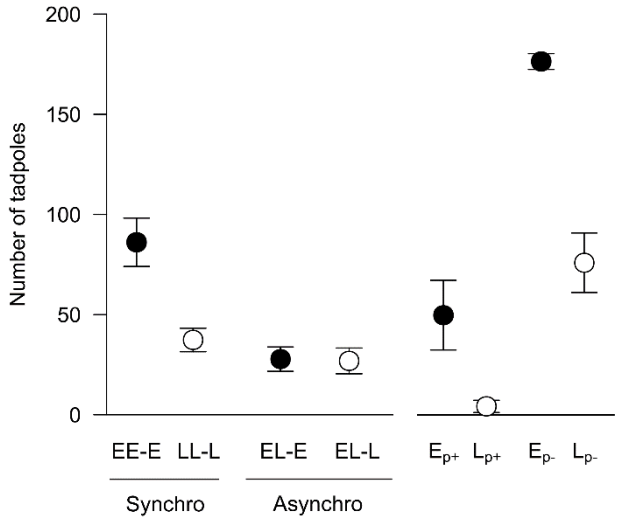

Fig. 8. The effects of treatments (synchrony/asynchrony), periods (early/late) and predator presence (or absence) on the mean survival rate (± SE) of tadpoles in each tank. The left four treatment types were same as the types shown in Fig. 6. E_{p+}, L_{p+}, E_{p-}, and L_{p-} denote predator presence in the early and late periods, and predator absence in the early and late periods, respectively.

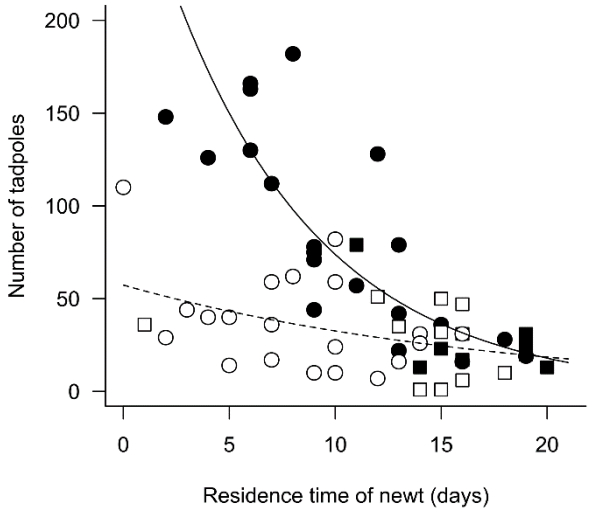

Fig. 9. The effects of the residence time of the newts on the number of surviving tadpoles in each tank. Solid and open circles represent tanks in synchronous treatments in the early and late periods, respectively, while solid and open squares denote tanks in an asynchronous treatment in the early and late periods, respectively. Solid and dotted lines are the prediction lines for the early and late periods respectively, with their interactions with the residence time. The predictions were based on the corresponding GLM analyses (see text for Results).

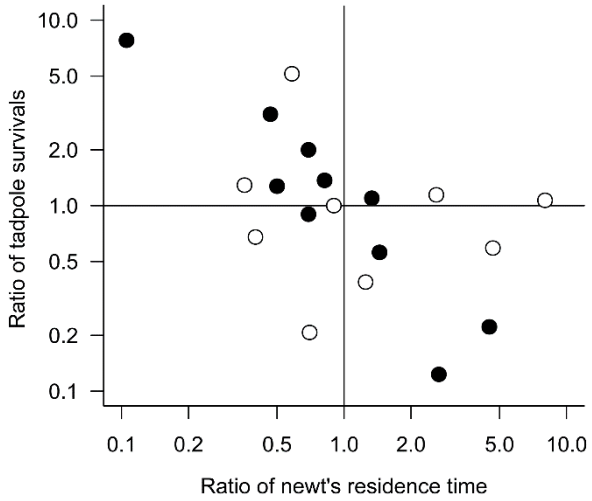

Fig. 10. The relationship between the ratio of newt's residence time and the ratio of tadpole survivals between the two tanks in a treatment enclosure. Solid and open circles are the early and late periods, respectively. Note that log scale was used in the panel.

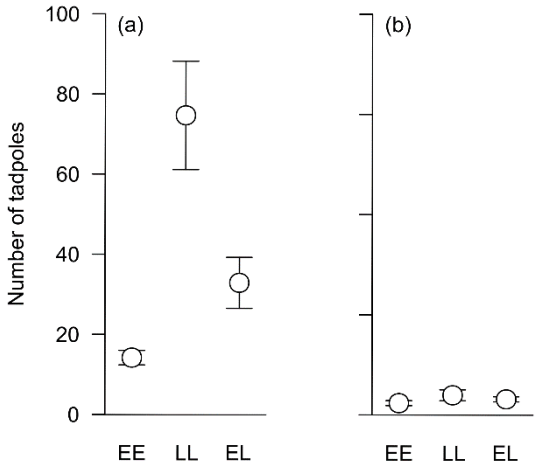

Fig. 11. The effects of treatments and periods on the total survival rate of tadpoles in each enclosure. The total number of surviving tadpoles counted (sum of the two tanks for an enclosure) at the end of the late period (a) and 23-days after the completion of the late period (b). Error bars represent SE.

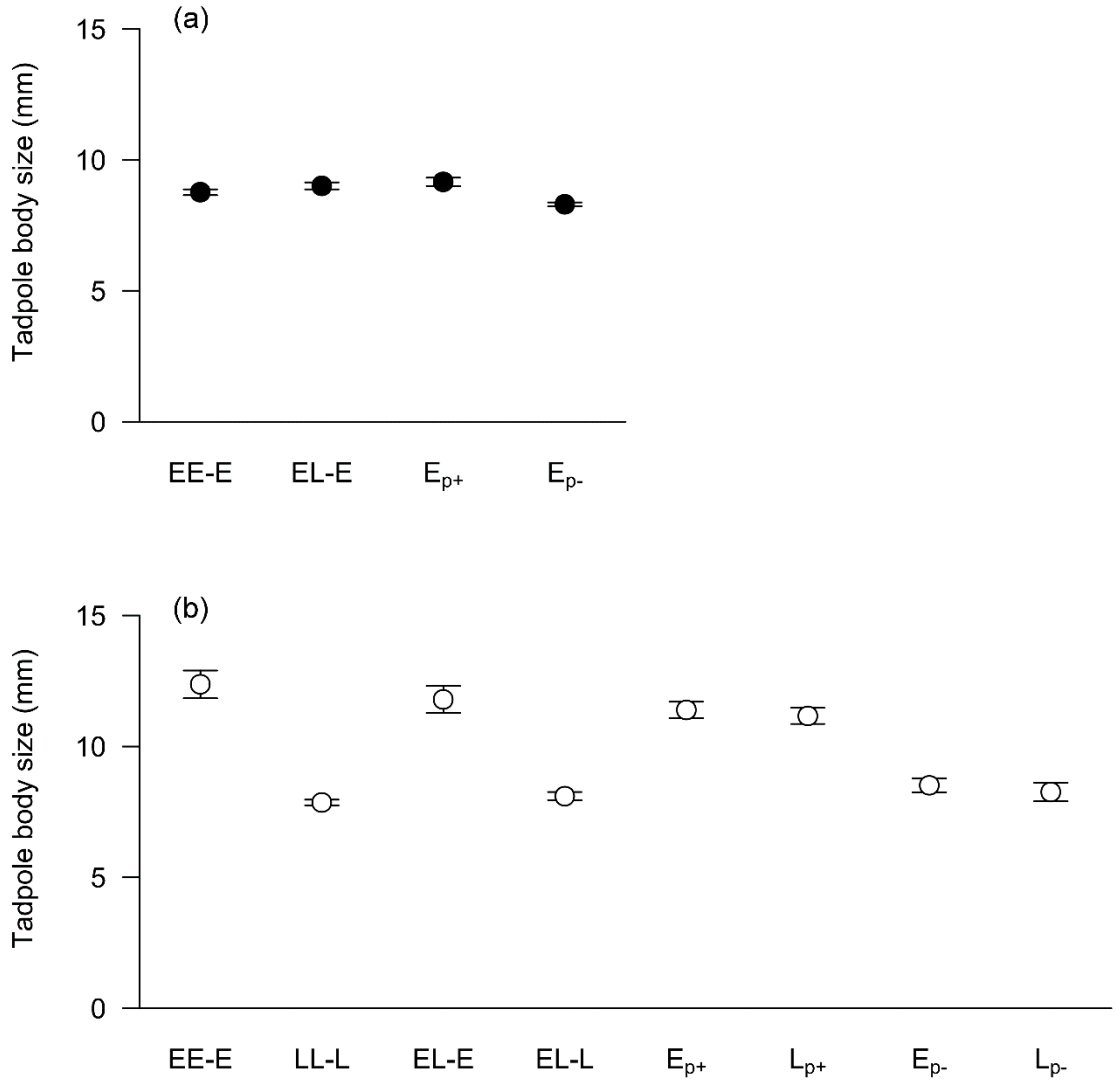

Fig. 12 Mean body size (Snout-Vent Length) of tadpole in the early (a) and late periods (b). Error bar represents a standard error of a mean value for each tank in each treatment.

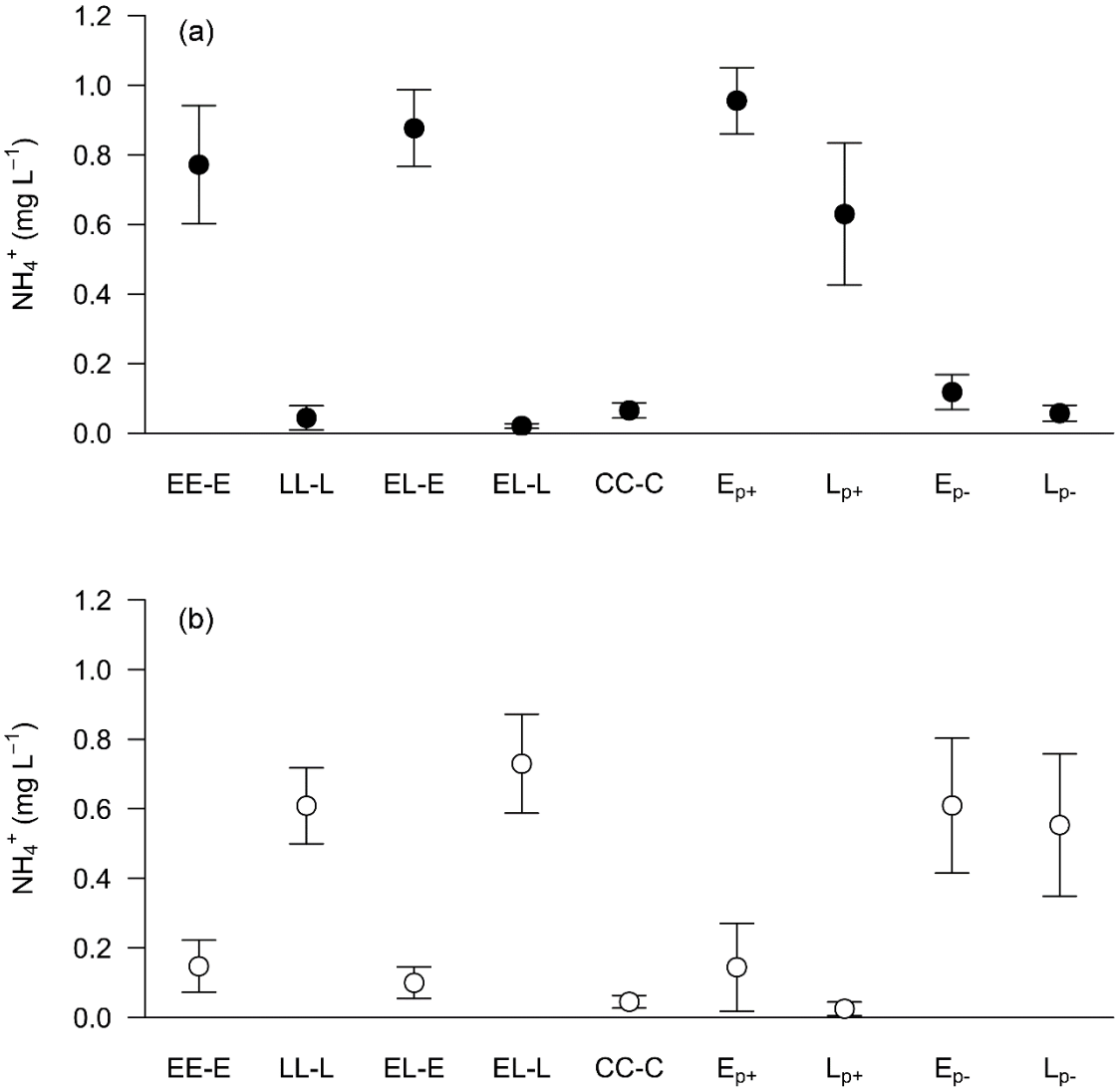

Fig. 13. Water NH_4^+ concentration in each tank in each treatment (Mean ± SE) on 6 July (a) and 30 July (b).

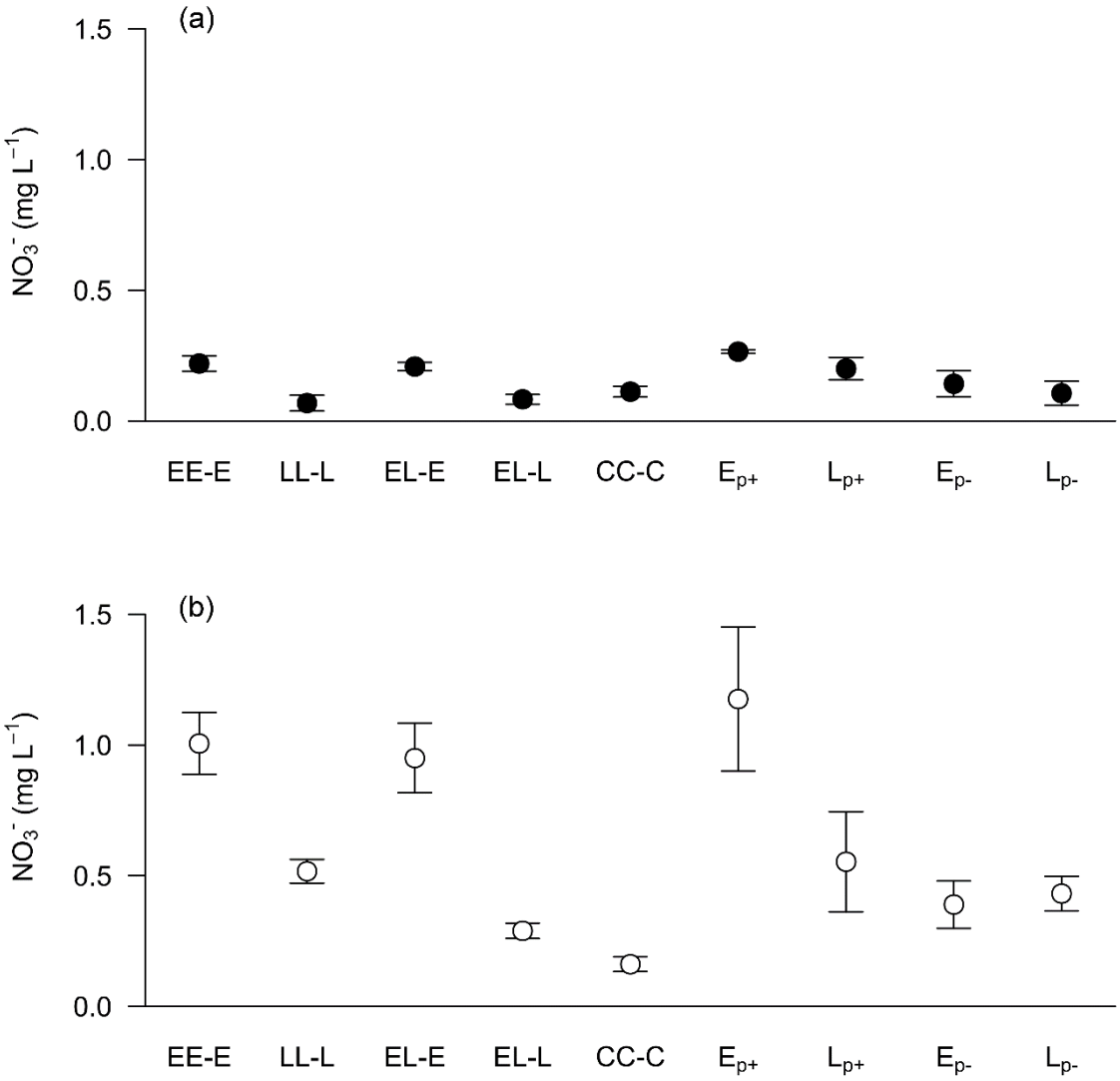

Fig. 14. Water NO_3^- concentration in each tank in each treatment (Mean ± SE) on 6 July (a) and 30 July (b).

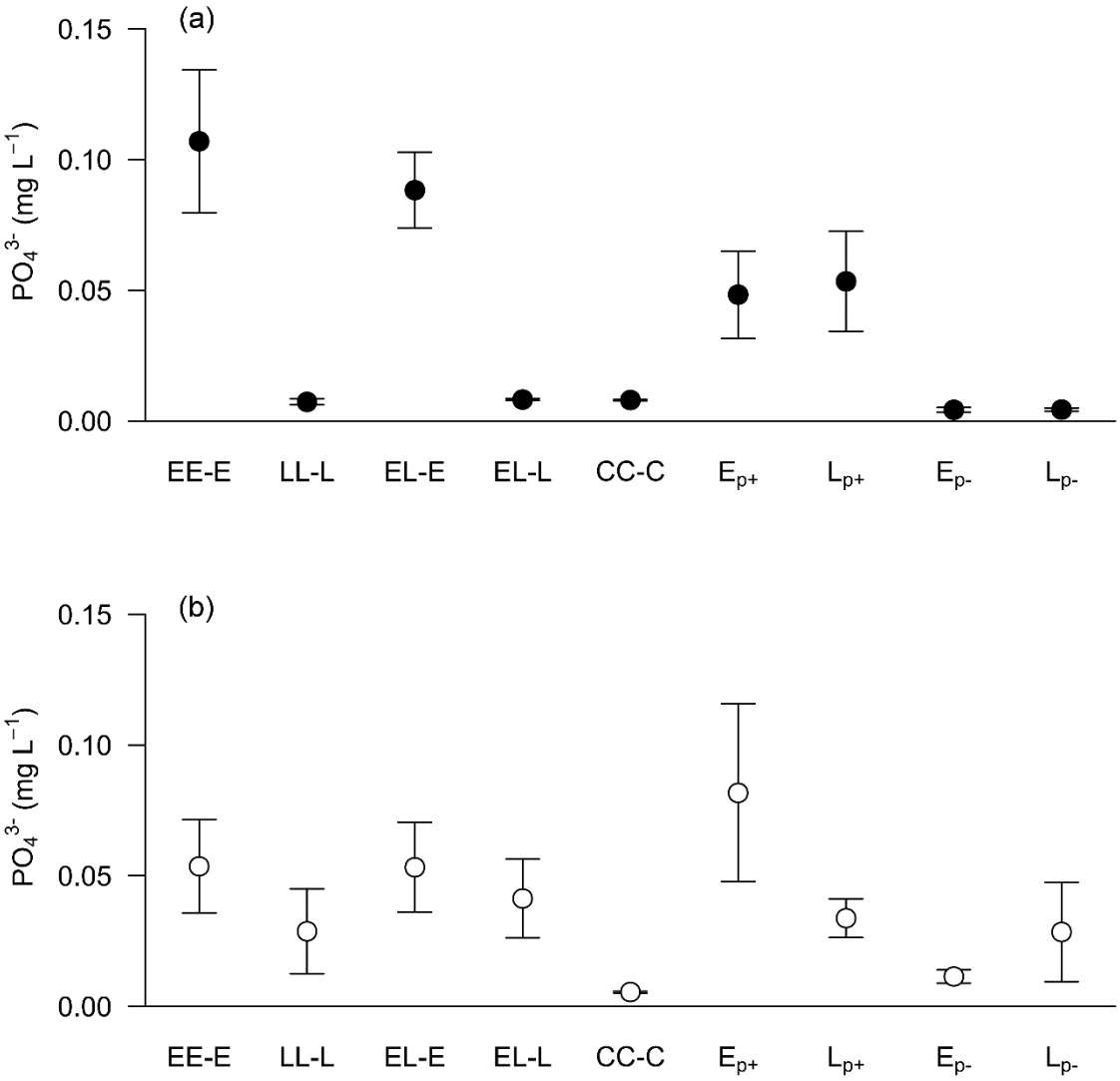

Fig. 15. Water PO_4^{3-} concentration in each tank in each treatment (Mean ± SE) on 6 July (a) and 30 July (b).

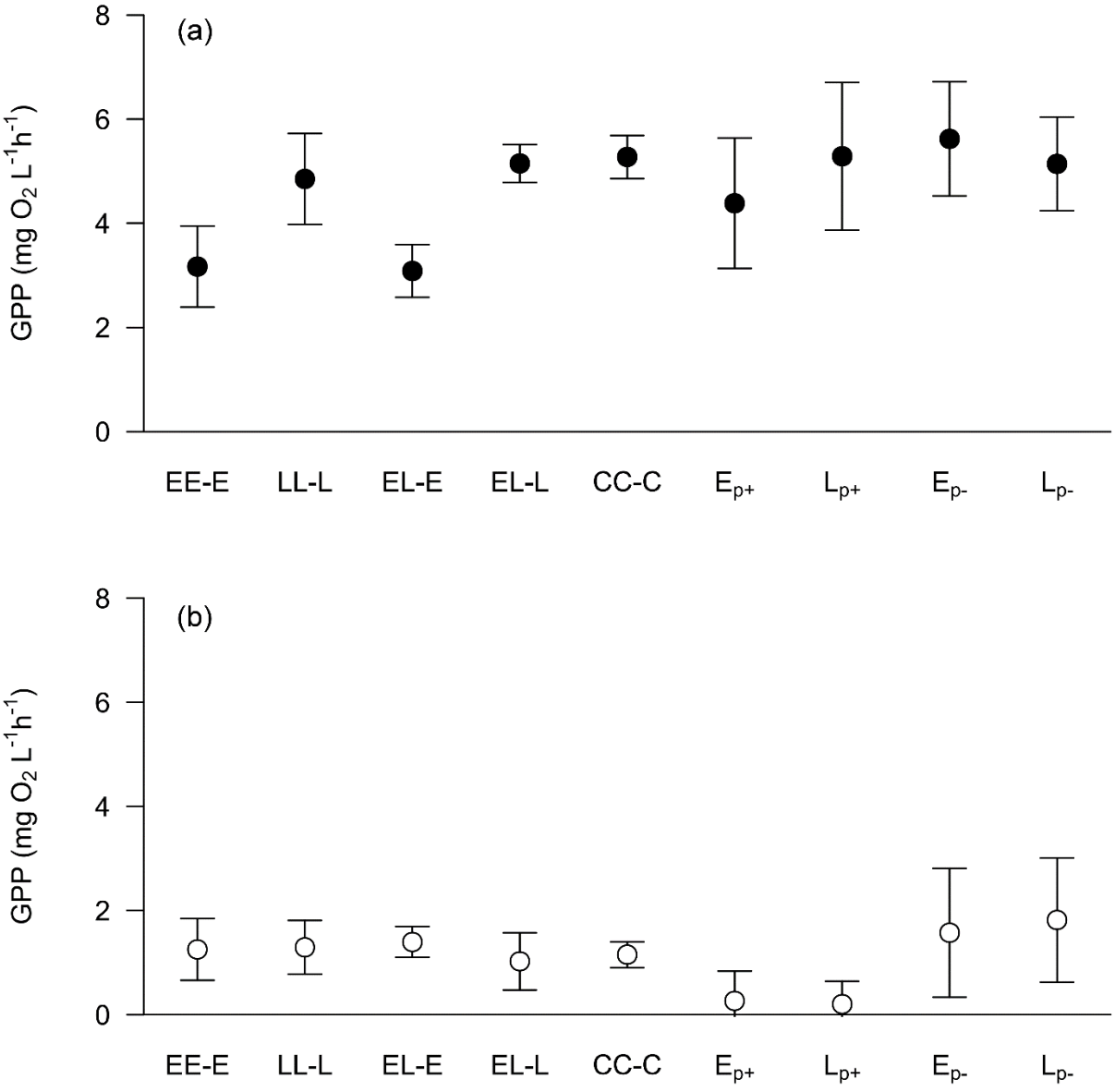

Fig. 16. Gross primary productivity (GPP) in each tank in each treatment (Mean ± SE) on 6 July (a) and 30 July (b).

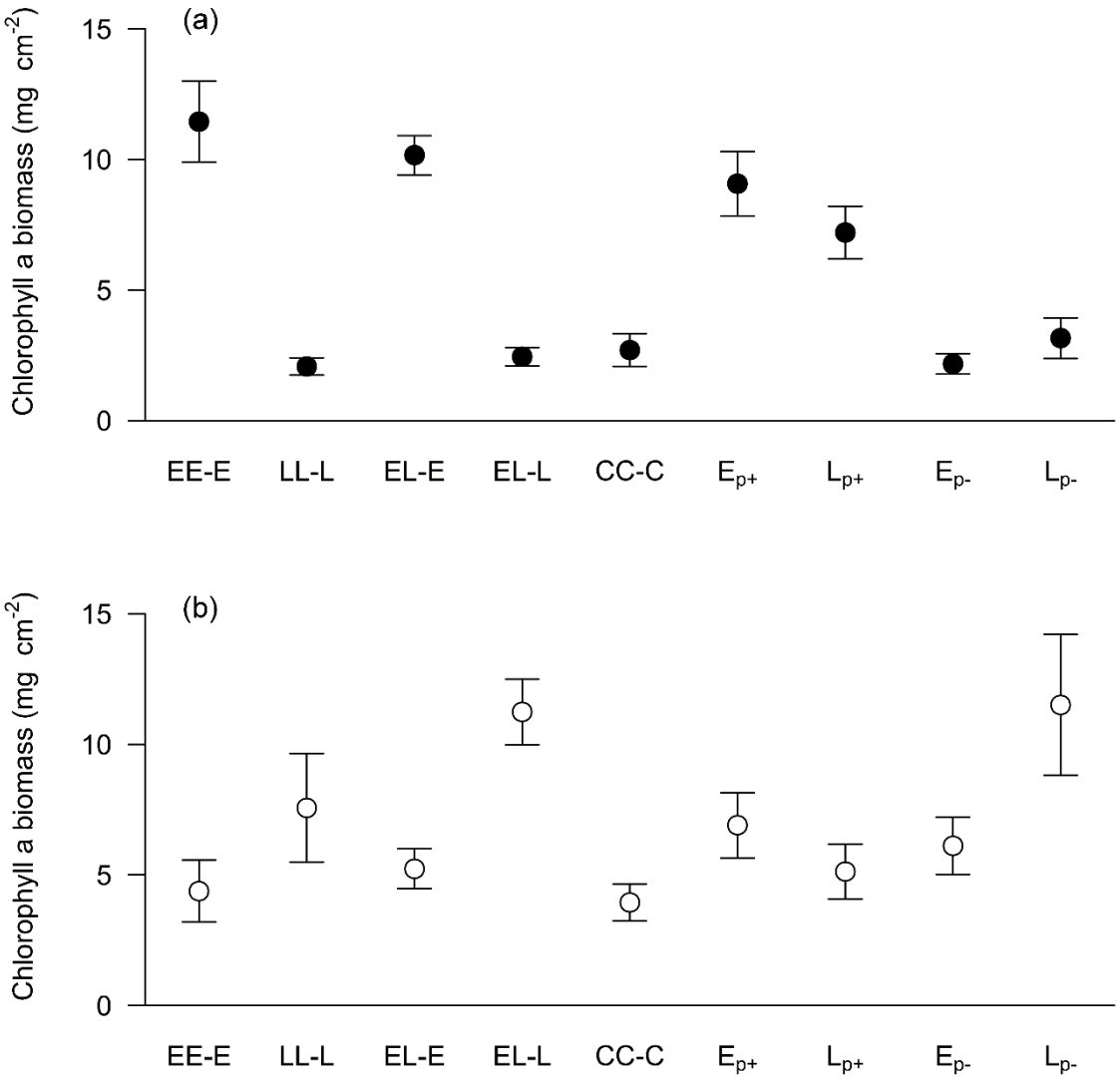

Fig. 17. Periphyton biomass in each tank in each treatment (Mean ± SE) on 9 July (a) and 31 July (b).

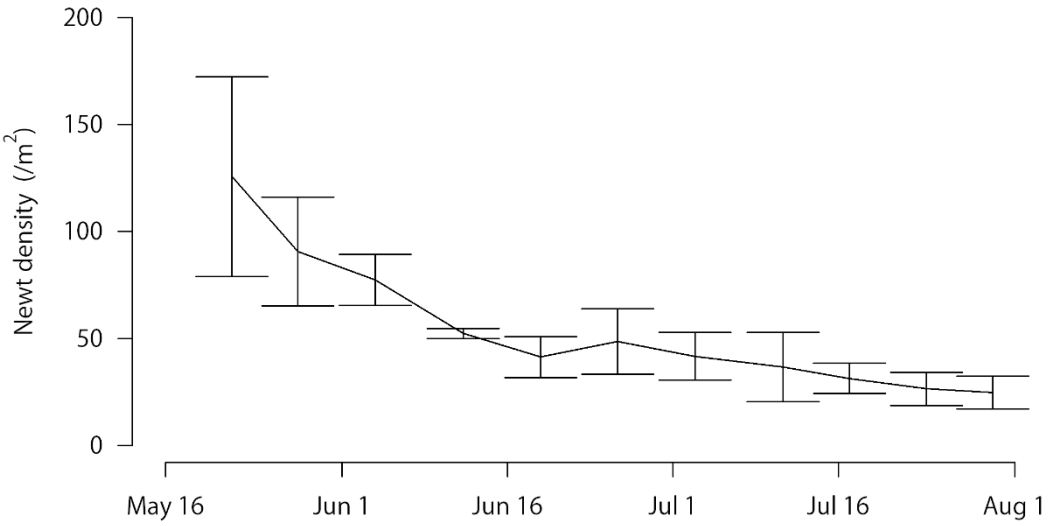

Fig. 18.

Seasonal density of *Cynops pyrrhogaster* in 2018 at AFRS (Mean ± SE). Field surveys were conducted at three sites (Site 1, 4, and 19). The density in each site was estimated by the removal method (Carle & Strub 1978).

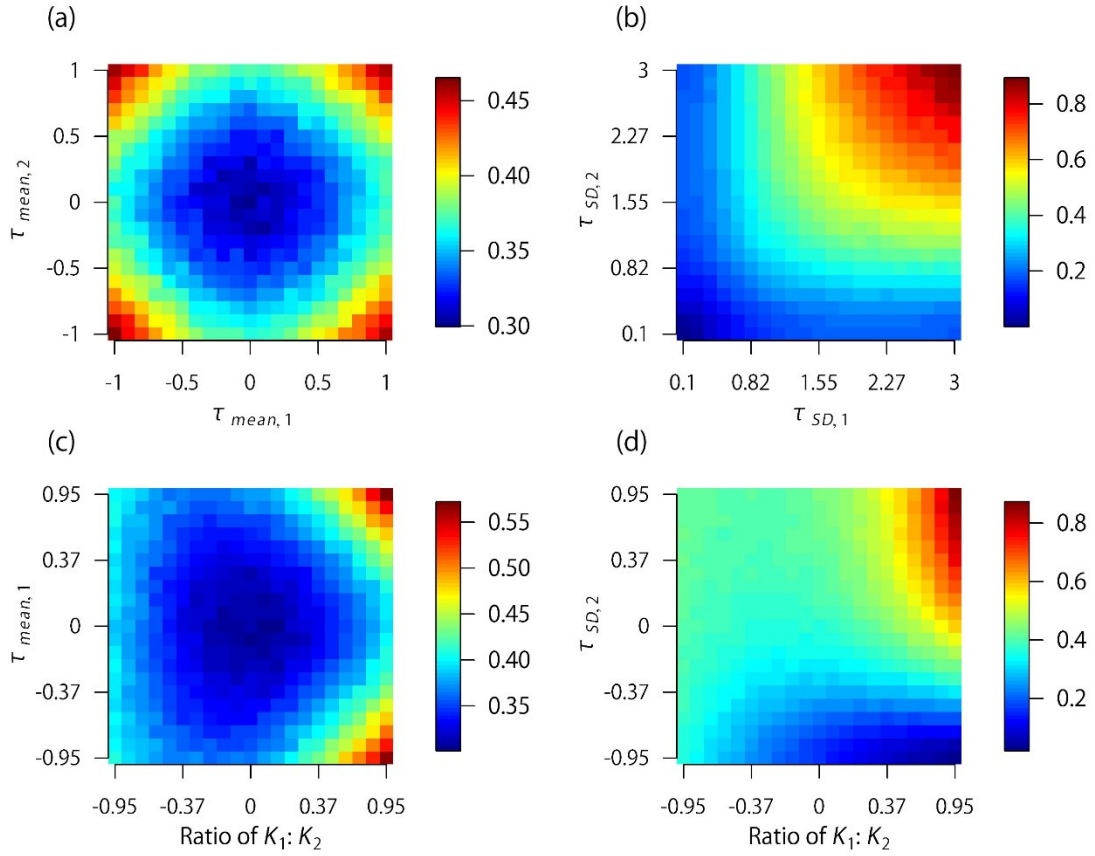

Fig. 19. Metapopulation stability: coefficient of variation (CV) of the total metapopulation abundance in the base model, (a) Each axis presents the mean phenological peak in each patch ($\tau_{mean,i}$); (b) variance of phenological peaks in each patch ($\tau_{SD,i}$); (c) common logarithm of the ratio of habitat size ($\log_{10}(K_1/K_2)$) versus mean phenological peak; (d) common logarithm of the ratio of habitat sizes versus variance of phenological peaks in each patch. Parameters re not shown in the axes are as follows: $K_1 = K_2 = 500$; $h = 0.9$; $C = 300$; $\alpha = 0.7$; $\beta = 1$; $\tau_{mean,1} = 0$; $\tau_{mean,2} = 0$; $\tau_{SD,1} = 1$; $\tau_{SD,2} = 1$; $m = 0.3$; $e_{21} = e_{12} = 0.1$.

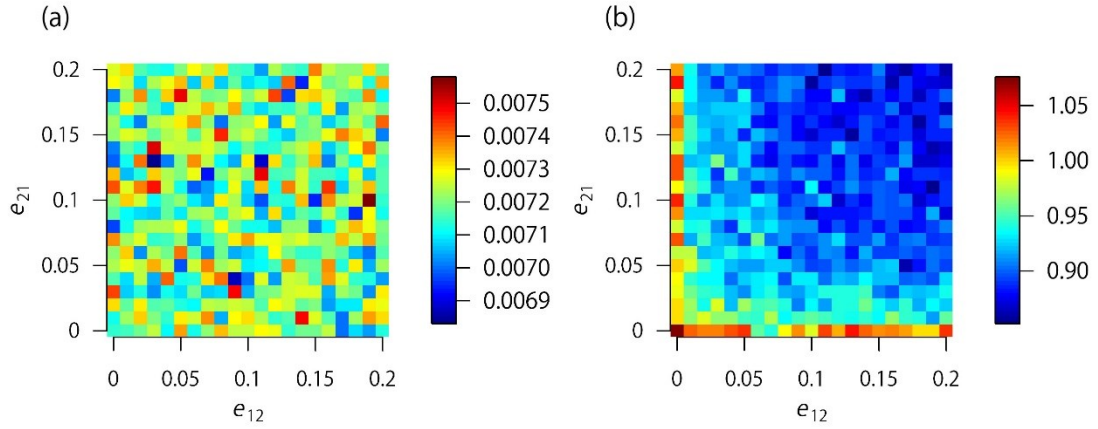

Fig. 20. Metapopulation stability: coefficient of variation (CV) of the total abundance in the base model. Each axis presents the migration rate from population i to population j (e_{ji}), (a) with small fluctuations in phenological peaks ($\tau_{SD,1} = \tau_{SD,2} = 0.1$) and (b) with large fluctuations in phenological peaks ($\tau_{SD,1} = \tau_{SD,2} = 3$). Parameters are as follows: $K_1 = K_2 = 500;\ h = 0.9;\ C = 300;\ \alpha = 0.7;\ \beta = 1;\ \tau_{mean,1} = \tau_{mean,2} = 0;\ m = 0.3$.

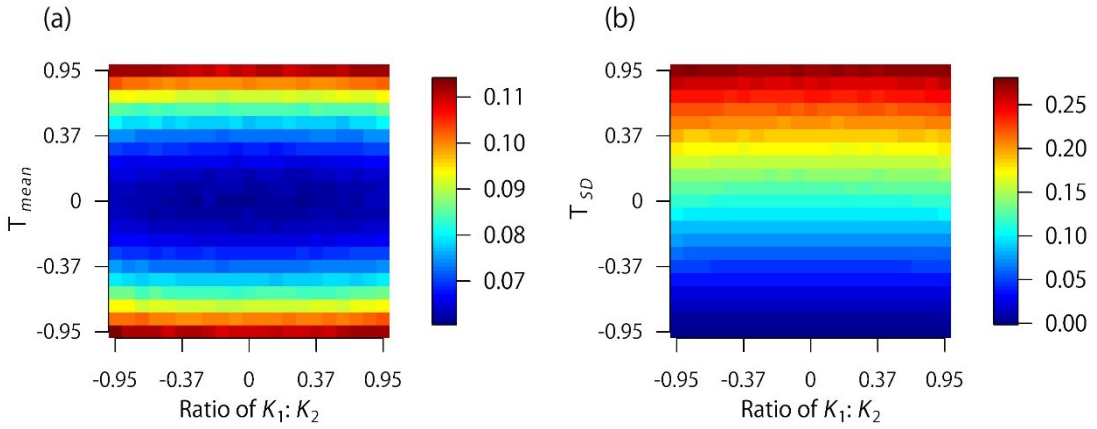

Fig. 21. Metapopulation stability: coefficient of variation (CV) of the total abundance in the demographic stochasticity model, (a) Each axis presents the common logarithm of the ratio of habitat sizes (K_i) versus the mean phenological peaks in the whole research site (T_{mean}); (b) the common logarithm of the ratio of habitat sizes ($\log_{10}(K_1/K_2)$) versus the variance of phenological peaks in the whole research site (T_{SD}). Parameters not shown in the axes are as follows: $h = 0.9$; $C = 300$; $\alpha = 0.7$; $\beta = 1$; $T_{mean} = 0$; $T_{SD} = 1$; $m = 0.3$; $e_{21} = e_{12} = 0.1$.

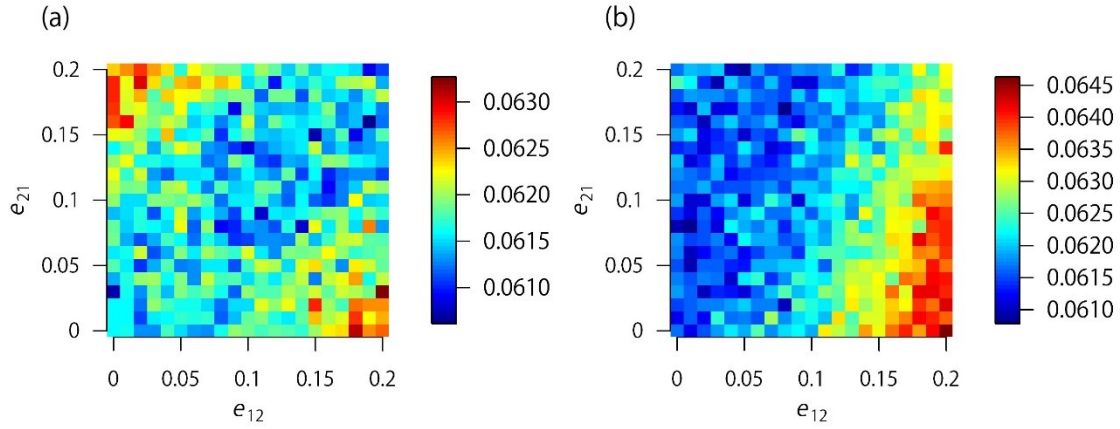

Fig.22. Metapopulation stability: coefficient of variation (CV) of the total abundance in the demographic stochasticity model. Each axis presents the migration rate from population i to population j (e_{ji}). (a) The habitat sizes are equal between the two populations ($K_1 = K_2 = 500$) and (b) the habitat sizes differed between the two populations ($K_1 = 750;\ K_2 = 250$). Other parameters are as follows: $h = 0.9;\ C = 300;\ \alpha = 0.7;\ \beta = 1;\ T_{mean} = 0;\ T_{SD} = 1;\ m = 0.3$.